Lake Clarke and Lake Aldred Sediment Transport Modeling

Final Report

Prepared by:

WEST Consultants, Inc.

May 2017

Lake Clarke and Lake Aldred
Sediment Transport Modeling

Final Report

May 2017

Prepared for:

Exelon Energy Corporation
300 Exelon Way
Kennett Square, PA 19348

Prepared by:

WEST Consultants, Inc.
11440 W. Bernardo Court, Suite 360
San Diego, CA 92127

WEST Project No. EWIN001-001

Cover Page Photo Credits (clockwise):
Seth Derr (2011), D. Haschert (n.d.), and TheGates1210 (2011)

EXECUTIVE SUMMARY

Recent interest in the impact of the Lower Susquehanna River reservoirs (Lake Clarke, Lake Aldred, and Conowingo Pond) on the transport of sediment and other watershed-based constituents, and, ultimately, on Chesapeake Bay water quality, has prompted a variety of research and modeling efforts. WEST Consultants, Inc. (WEST) was contracted by Exelon Corporation (Exelon) to develop a one-dimensional, fully-unsteady HEC-RAS 5.0 sediment transport model of Lakes Clarke and Aldred as part of a multi-model initiative spanning these two reservoirs plus Conowingo Pond. The model was hydraulically calibrated using stage and discharge data from the United States Geological Survey (USGS) streamgage at Marietta, PA (USGS Gage No. 01576000), and calibrated for sediment transport using observed bed volume change for both reservoirs between 2008 and 2013. Modelers used a verification period from 2013 to 2015 to validate the model's performance during a time characterized by lower flows. The calibrated model successfully replicated bed changes for both reservoirs and time periods within target ranges defined by survey equipment accuracy, and simulated both deposition and scour processes at varying discharges and reservoir states. Sediment rating curves were developed for three particle size classes (sand, silt, and clay) at the upstream boundary at Marietta, at Safe Harbor Dam (impounding Lake Clarke), and at Holtwood Dam (impounding Lake Aldred). The curves were provided to the Chesapeake Bay Program to aid in parameterization of the Chesapeake Bay Watershed Model, and a time series of discharge and sediment loading at Holtwood Dam was provided to HDR, Inc. (HDR) for use as input to their three-dimensional Conowingo Pond Mass Balance Model.

TABLE OF CONTENTS

LIST OF TABLES

LIST OF FIGURES

LIST OF APPENDICES

1 INTRODUCTION

1.1 PROJECT BACKGROUND

As the largest tributary to the Chesapeake Bay (the Bay), the Susquehanna River plays a primary role in supplying fresh water, sediment and nutrients to the Bay system. Recent concern about storm-driven sediment and associated nutrient pulses, which can negatively affect Bay ecosystems and related industries, resulted in ongoing collaborative work between a wide consortium of public and private agencies and organizations. In addition to focus on land use and wider watershed management, attention was given to the role of three Lower Susquehanna hydroelectric dams in regard to sediment and nutrient flux dynamics. The dams—Safe Harbor, impounding Lake Clarke; Holtwood, impounding Lake Aldred; and Conowingo, impounding Conowingo Pond—which for many decades served as net sediment traps, are generally believed to have approached or reached states of dynamic equilibrium. In this state, the volume of stored sediment may oscillate in the short term, but is relatively stable when averaged over the long term. Based on the current understanding of the system, some large storms may, in addition to importing new sediment from the watershed, also scour previously-deposited sediment in the reservoirs. The dams are not themselves sources of sediment—that is, they do not create or produce sediment, but rather trap, store, and release sediment sourced from the watershed at intervals determined by the states of the reservoirs, the frequency and magnitude of storm events, and the magnitude of inflowing sediment loads. Most recent research has considered the role of Conowingo Dam, which impounds the last of the three reservoirs with some remaining sediment trapping capacity. The present study focuses on Safe Harbor and Holtwood Dams, which together impound approximately 20 miles of the Lower Susquehanna River between Marietta, PA and Holtwood, PA.

Safe Harbor Dam was constructed in 1931, and its average height of 75 feet (ft.) produced a usable design storage of approximately 3,000,000,000 cubic feet (ft^3; about 69,000 acre-ft.) over an area of about 7,360 acres. The dam is operated by the Safe Harbor Water Power Corporation (SHWPC) (Safe Harbor Water Power Corporation, n.d.). Construction of Holtwood Dam was completed in 1910, and with a height of 55 ft., the structure impounds a 2,400-acre reservoir (Porse, 2010). Ownership and operation of the dam transferred to Brookfield Renewable Energy Partners in April 2016 (Weissman, 2016).

The Susquehanna River Watershed has been the subject of considerable research in recent years. In 2010, the United States Environmental Protection Agency (EPA) established total maximum daily load (TMDL) limits for sediment and nutrients supplied to the Chesapeake Bay (USEPA, 2010), which prompted formation of a plan by The District of Columbia, Maryland, Pennsylvania, Virginia, New York, West Virginia, Delaware, the Chesapeake Bay Commission, and the EPA to reduce fluxes. The political, ecological, and financial implications of the plan prompted a marked

increase in studies focused on the reservoir and Bay systems, many of which were still in process at the time of writing.

Past studies of the Lower Susquehanna reservoir system included physical and chemical profiling of the reservoirs' bed sediments (Hainly, et al., 1995; Reed & Hoffman, 1996; Ott, et al., 1991; Takita & Edwards, 2001; Edwards, 2006), computations of changes in dam storage capacities and trap efficiencies (Hainly, et al., 1995; Langland, 2009), evaluation of the hydrodynamic impacts on deposition and scour rates (Hainly, et al., 1995; Langland & Koerkle, 2014; Hirsch, 2012), and other important topics.

1.2 STUDY PURPOSE

Exelon contracted WEST to develop an unsteady, one-dimensional sediment transport model of the upper two reservoirs, ultimately to help parameterize the Chesapeake Bay Watershed (HSPF) Model and provide inputs for a three-dimensional sediment and nutrient flux model developed by HDR for Conowingo Pond. The choice to model sediment fluxes was made within the context of the larger Integrated Monitoring Program: originally, Gomez & Sullivan Engineers planned to collect gaged inter-reservoir sediment data as part of Exelon's Lower Susquehanna River Integrated Sediment and Nutrient Monitoring Program, but insufficient data were collected due the absence of large storm events during the program's duration. The purpose of this study was to develop improved understanding of sediment transport processes in Lakes Clarke and Aldred through use of a deterministic numerical model, the U.S. Army Corps of Engineers (USACE) Hydrologic Engineering Center-River Analysis System (HEC-RAS), in lieu of observed sediment transport data.

While other sediment transport models, including HEC-RAS, were previously developed for the same reach, the current study aimed to build and improve upon earlier work with a new version of the model, HEC-RAS v. 5.0, which was officially released in March 2016. Version 5.0 offers several key advantages over previous HEC-RAS versions. Instead of approximating the hydrodynamics as a series of steady flows (a quasi-unsteady simulation), as was the case in earlier versions, the model's new, fully-unsteady sediment transport capabilities solve the unsteady flow equation, routing flow through the model and explicitly accounting for storage and travel time. Volume is thus conserved, which is very important in reservoir systems. Other improvements include features designed to add more flexibility and precision to sediment inputs, such as the ability to input sample-specific cohesive parameters for bed gradations. A more detailed description of the model is given in Section 2.

1.3 STUDY AREA

The study area extends along the Susquehanna River from near the town of Marietta, PA, to Holtwood Dam near Holtwood, PA (see Figure 1.1). The HEC-RAS model encompasses the study area and includes contributions from three significant tributaries: Chiques Creek, Conestoga River, and Pequea Creek.

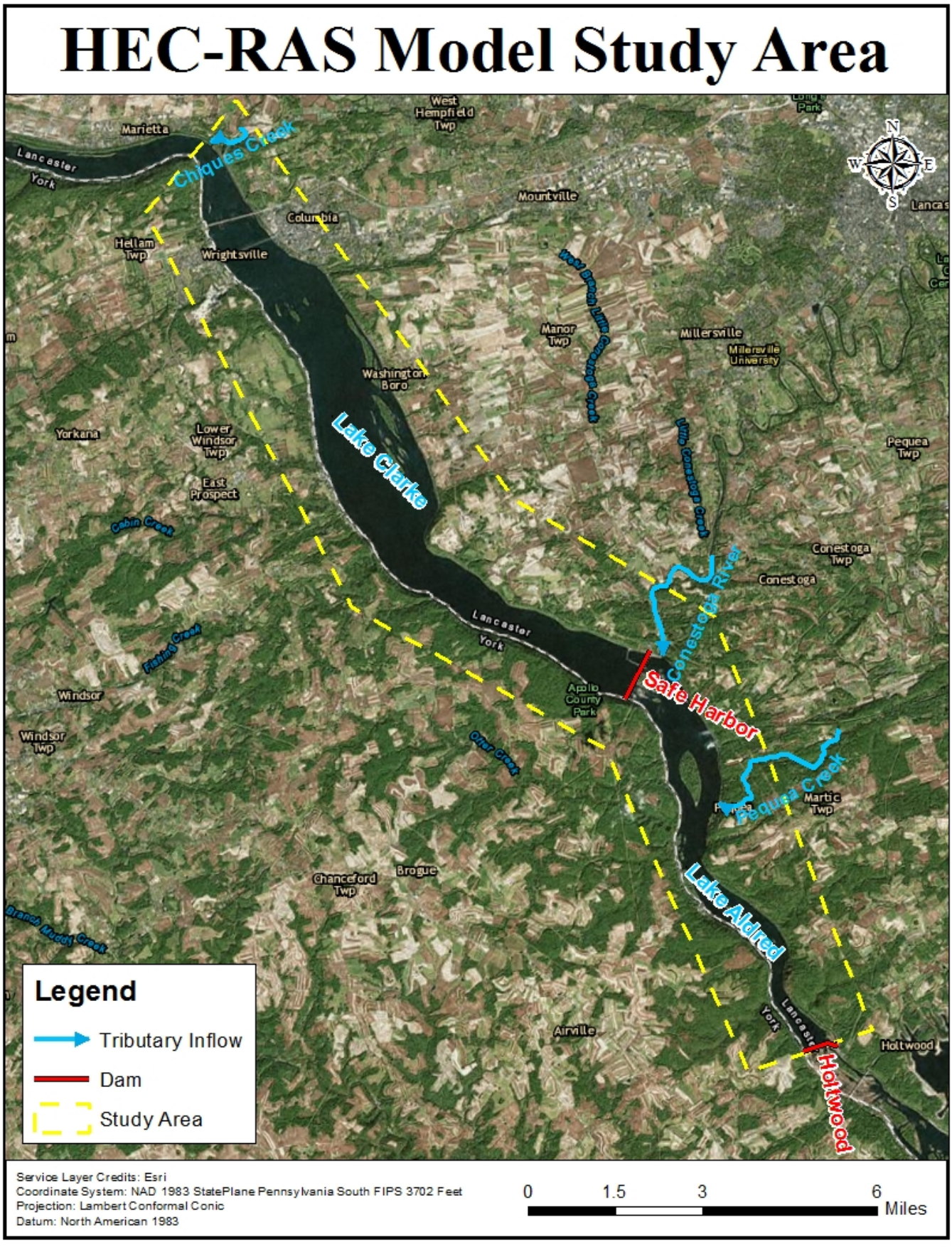

Figure 1.1. HEC-RAS Model Study Area

1.4 PREVIOUS STUDIES

Given the scope of the current project, the following review is limited to recent models and studies which attempted to simulate or directly observe sediment transport dynamics throughout the reservoir system. Hainly, et al. (1995) developed a quasi-unsteady USACE HEC-6 Model from Marietta, PA to Conowingo Dam, which was calibrated to 1987 calendar year flows and verified using 1988-1989 storm events. Both cohesive and non-cohesive sediments were modeled. Despite the fairly high quality of input data, the model computed a low trap efficiency compared to the measured trap efficiency over the entire system. To compensate, the inflow sediment sizes were coarsened significantly.

Gomez and Sullivan Engineers and URS Corporation (Exelon, 2012) used the HEC-6 model developed by Hainly et al. (1995) to test three hypotheses:

1) 400,000 cubic feet per second (cfs) is the trigger flood event for net scour;

2) Safe Harbor and Holtwood Dams are at dynamic equilibrium; and

3) Tropical Storm Agnes resulted in a major net scour event in Conowingo Pond.

The report prepared by Gomez and Sullivan and URS Corporation (URS) (Exelon, 2012) concluded the following regarding these hypotheses:

1) The HEC-6 analysis contradicts the scour regression model which is predicated on a 400,000 cfs scour threshold;

2) The HEC-6 model suggests that Lake Clarke is not in dynamic equilibrium and Safe Harbor Dam is trapping sediment;

3) The HEC-6 analysis does not seem to support the conclusion within the literature that the catastrophic impact to Chesapeake Bay from Agnes was due to scour from Conowingo Pond.

After reviewing the existing literature and HEC-6 results, URS and GSE (2012) identified a need for a comprehensive and integrated analysis of the Lower Susquehanna River watershed and all three lower river reservoirs, noting that the USACE was undertaking such a study as part of the Lower Susquehanna River Watershed Assessment (LSRWA).

As part of the LSRWA, Langland and Koerkle (2014) developed a quasi-unsteady USACE HEC-RAS Model (v. 4.2 beta 2012-07-19) from Marietta, PA to Conowingo Dam, using cross-sections based in part on 2008 surveyed bathymetry. The model was run from 2008 to 2011 and was unable to accurately simulate both depositional and scour processes. As a result, two models were developed: one calibrated to simulate net deposition over the 2008-2011 period, using computed bed volume changes and measured sediment outflows at Conowingo Dam, and one to simulate estimated net scour during Tropical Storm Lee in September 2011.

In addition to past attempts to model sediment transport dynamics, in 2014 Exelon, the Maryland Department of Natural Resources (MDNR), the Maryland Department of the Environment (MDE), USACE, the EPA, the Chesapeake Bay Program, the USGS, and the University of Maryland Center for Environmental Science (UMCES) developed a comprehensive sediment and nutrient monitoring program in an effort to develop new understanding about the flux of sediment and associated nutrients throughout the reservoir system. This program is the Lower Susquehanna River Integrated Sediment and Nutrient Monitoring Program (Integrated Monitoring Program). Sampling stations were established at Marietta, PA and at all three dams to directly measure sediment and nutrient dynamics and to help provide a fuller picture of the dependence of fluxes on discharge. However, as of March 2016 only two official sampling events had occurred, both of which had peak flows less than 182,000 cfs. Due to a lack of storm events in the target flow range and the lack of available corresponding empirical data, in late 2015 program partners began discussing alternative approaches that could be implemented in early 2016 to supplement the modeling efforts associated with the Chesapeake Bay TMDL 2017 Midpoint Assessment.

1.5 PROJECT AUTHORIZATION AND ACKNOWLEDGEMENTS

This study was performed for the Exelon Corporation by WEST Consultants, Inc. Kimberly Long, the Exelon Project Manager for this study, provided support throughout the modeling effort.

Martin J. Teal, P.E., was the WEST Consultants project manager and technical lead. Jonathan Viducich provided the majority of the technical analyses performed. Rosa Aguilar worked on the volume change analysis and Sam Powvall provided GIS support.

Tim Sullivan, Gary Lemay, P.E., and Tom Sullivan, P.E., of Gomez and Sullivan Engineers provided technical input as well as the bathymetric data and volume change calculations used in the calibration and verification processes.

2 MODEL DEVELOPMENT

WEST prepared a numerical model to simulate hydraulic and sediment transport processes in Lake Clarke and Lake Aldred. This chapter describes the selected model software and input data to the model. Model results as well as limitations are presented in subsequent chapters.

2.1 THE HEC-RAS MODEL

The USACE's HEC-RAS is an integrated software package designed to perform one-dimensional steady and unsteady hydraulics analyses, two-dimensional steady and unsteady hydraulics analyses, sediment transport computations, and water temperature and water quality modeling. The system is comprised of a graphical user interface (GUI), separate analysis components, data storage and management architecture, graphics, and reporting facilities (USACE, 2016b).

The first version of HEC-RAS was released in July 1995, with the most recent, 5.0, released in March 2016. The software was developed at HEC under the direction of Mr. Gary Brunner.

2.2 GEOMETRIC DATA

Lake Clarke and Lake Aldred were modeled using one-dimensional flow simulations in HEC-RAS version 5.0. HEC-RAS performs one-dimensional hydraulic calculations by solving the one-dimensional energy equation and/or momentum equation for flow through a channel comprised of two-dimensional cross-sections separated by known reach lengths. Definition of the channel's shape and roughness allows the model to solve for energy losses due to friction and contraction/expansion.

Langland and Koerkle's HEC-RAS model incorporated geometry based on a combination of 1996 and 2008 surveyed bathymetric data, LiDAR data, a historic flood insurance study, and hand-interpolated cross-sections (Langland & Koerkle, 2014; Sullivan, 2016a; MDNR, 2014). In lieu of more reliable and complete datasets, Langland and Koerkle's geometry was adopted as a starting point for model geometry development.

Holtwood Dam was replaced with an interpolated cross-section at the same location, and all downstream cross-sections and the Conowingo Dam structure were removed from the model. Langland and Koerkle placed their model's upstream boundary approximately 1.3 miles (mi.) upstream of the actual location of the Marietta streamgage, and given the lack of discharge, stage, and sediment data at that original upstream boundary location, the upper two cross-sections were removed for the current model (i.e., the upstream boundary of the model was placed at the true Marietta gage location).

Unlike the rest of the 2008 model geometry, the USGS-surveyed bathymetry for Lake Aldred was originally based on a water surface elevation referenced to a local Holtwood vertical datum, rather than the National Geodetic Vertical Datum of 1929 (NGVD29); (Sullivan, 2016a). To convert the geometry to a common datum (NGVD29), the elevation of each cross-section between Safe Harbor and Holtwood Dams was increased by 0.77 ft. (e.g., elevation 165.0 ft. Holtwood Datum equals elevation 165.77 ft. NGVD29).

The river stationing of some cross-sections was adjusted slightly, based on GIS analysis of their locations along the stream centerline. Levees and ineffective flow areas were added at several locations to better represent open channel flow dynamics within the channel. Figure 2.1 presents an X-Y-Z perspective plot of the model geometry showing the locations of levees and ineffective flow areas.

In all, the adjusted model covers a longitudinal distance of approximately 20.4 mi., represented by 43 cross-sections including the inline structure at Safe Harbor. The cross-sections' river stationing (RS) is based on their river distances upstream of Conowingo Dam in feet, following the convention used by Langland and Koerkle (2014) in their model. Figure 2.2 presents a schematic of the HEC-RAS model geometry; note that while the map shows the location of Holtwood Dam, the structure itself is not explicitly included in the model.

Manning's roughness coefficients (*n* values) from the Langland and Koerkle (2014) model were initially assumed, and some horizontal variation in *n* values was added to account for vegetated islands and other channel features visible in satellite imagery. The effect of channel roughness on flow varies inversely with stage—deeper flows in reservoirs are generally less sensitive to Manning's *n* values than are normal channel flows. Flow roughness factors (1 to 1.2) were applied to compensate for decreasing roughness associated with increasing depth between the Marietta streamgage (RS 187225.3) and the cross-section located between Wrights Ferry and the Veterans Memorial (Columbia-Wrightsville) Bridges (RS 179019). Seasonal roughness change factors (0.8 to 1.7) were also applied at the same locations to account for changes in bed roughness. When both flow and seasonal roughness factors are used, HEC-RAS first applies the flow adjustment, and then the seasonal roughness factor.

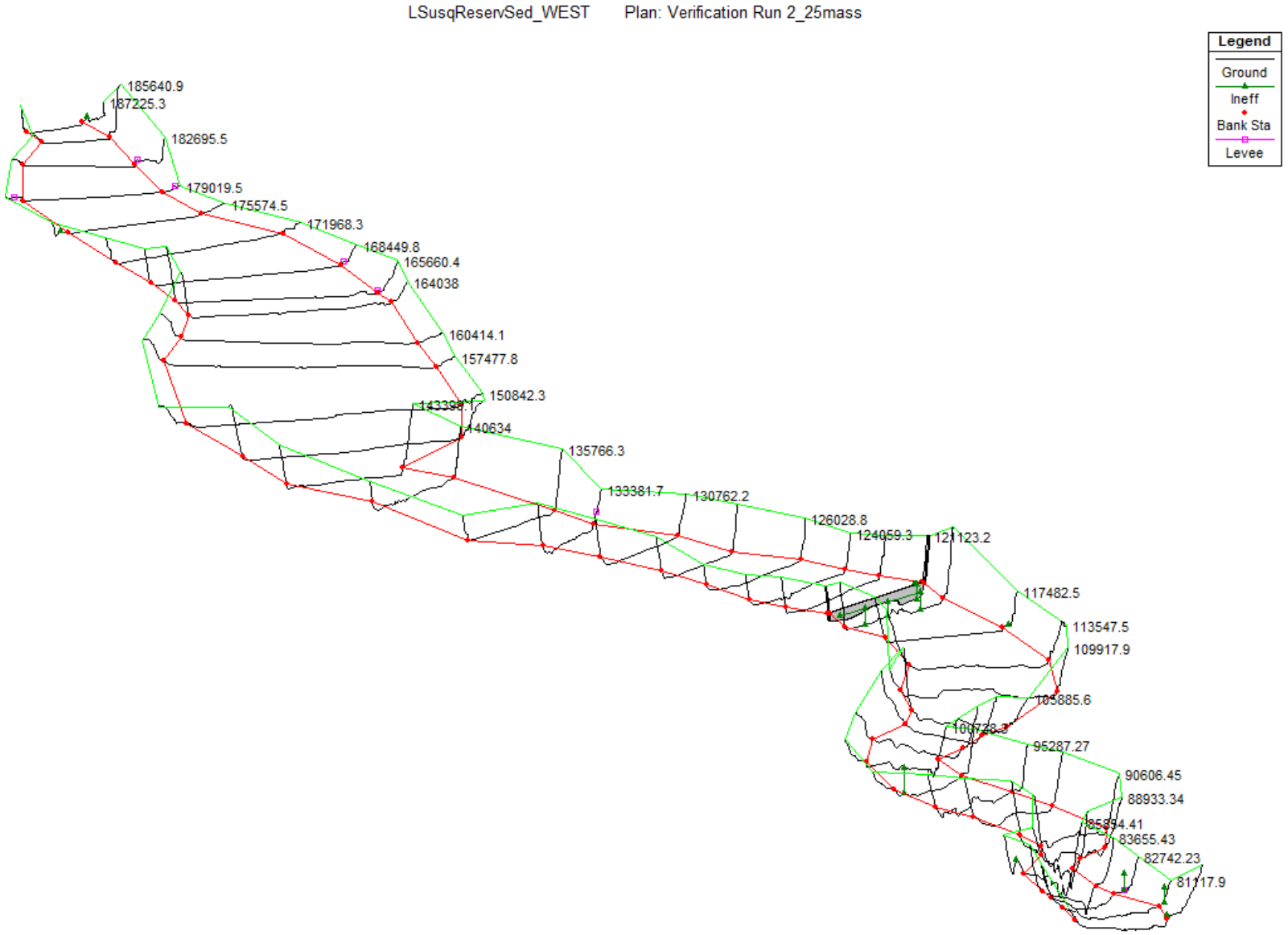

Figure 2.1. X-Y-Z Perspective Plot of Model Reach

HEC-RAS Model Schematic

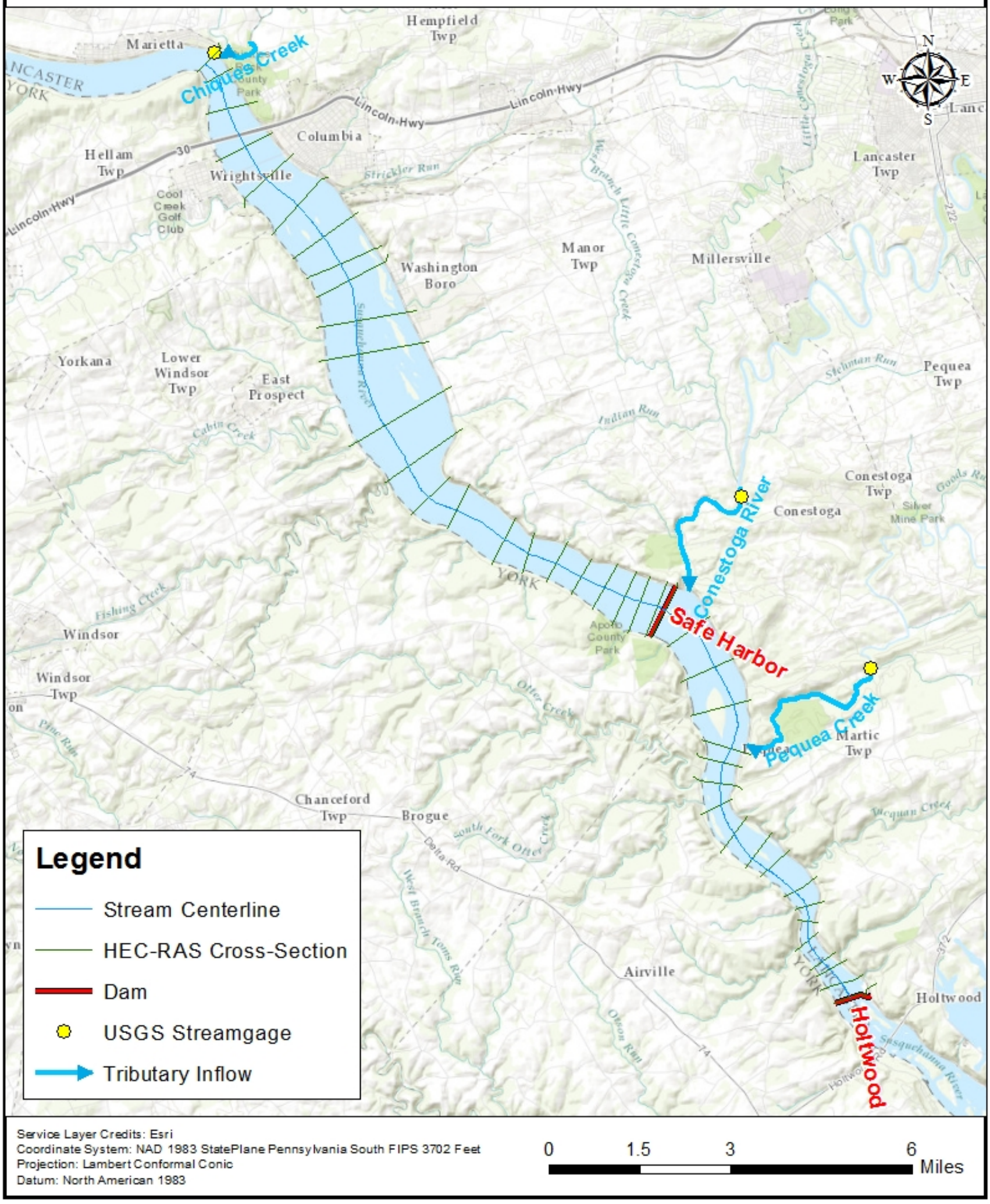

Figure 2.2. HEC-RAS Model Schematic

2.3 FLOW DATA

HEC-RAS requires a boundary condition to determine flow at the most upstream cross-section of a model, and additional inflows and other boundary conditions may be added at other locations. For the Lake Clarke and Lake Aldred HEC-RAS model, boundary condition discharges accounted for the flow contributions of the Susquehanna River and three tributaries: Chiques Creek[1], Conestoga River, and Pequea Creek. Together, the inflows account for 99.5% of the drainage area at Holtwood Dam.

A USGS streamgage (USGS 01576000) located on the Susquehanna River at Marietta, PA provided the upstream flow boundary condition. The gaged drainage area, which includes that of Chiques Creek, is approximately 25,990 square miles (mi^2). Flow data are available from the USGS website (USGS, 2016a) at 30-min time steps, and a 1-hour time series was developed for the full simulation period. Gaps in the data were interpolated using the HEC-RAS Interpolate Missing Values tool. Figure 2.3 shows the hourly input flow hydrograph measured at the Marietta gage. A maximum discharge of 665,000 cfs was recorded on 9 September 2011, as a result of Tropical Storm Lee, and a minimum flow of 3,720 cfs was recorded on 23 October 2008.

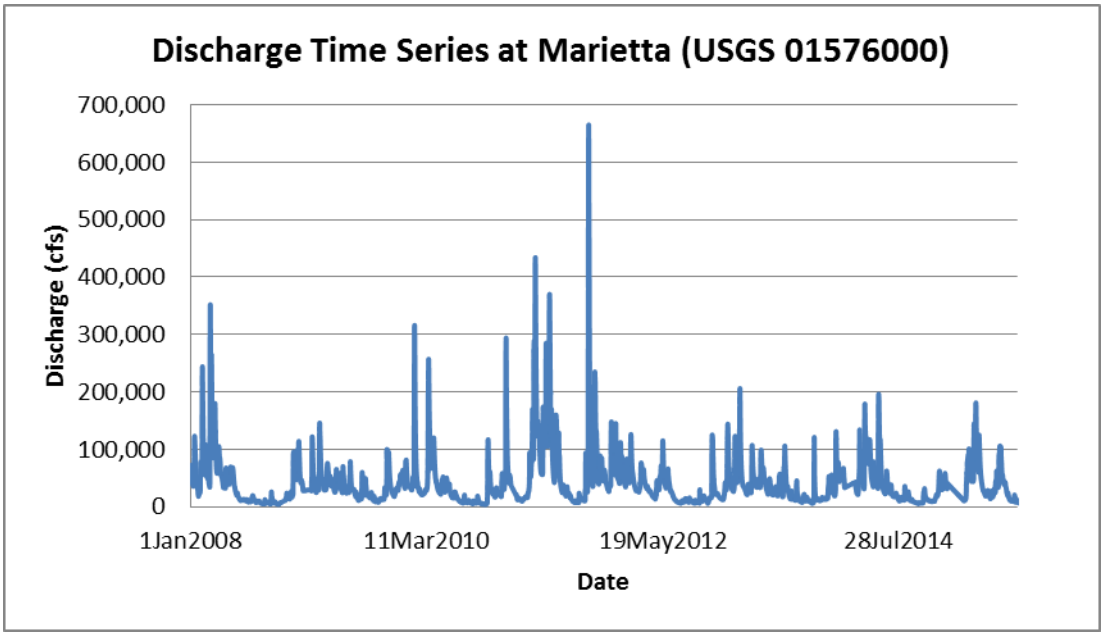

Figure 2.3. Discharge Time Series at Marietta, PA Streamgage

Lateral inflow data from the USGS streamgage (USGS 01576754) on the Conestoga River at Conestoga, PA were applied at model cross-section RS 117482.5, just downstream of Safe Harbor Dam. At that location, the drainage area of the Conestoga River is approximately 470 mi^2. The gaged discharge data are available

[1] Formerly "Chickies Creek"; the name was officially changed by the USGS in 2002. See http://geonames.usgs.gov/apex/f?p=gnispq:3:0::NO::P3_FID:1171772

for download at 15-minute intervals, and were converted to a 1-hour time series with a few small gaps interpolated.

A USGS streamgage (USGS 01576787) at Martic Forge, PA provided the lateral inflow data for Pequea Creek, which has a drainage area of 148 mi^2 at the gage and enters the Susquehanna River about 5 miles upstream of Holtwood Dam. Discharge data are available as 24-hour average values, and were used to create a 24-hour time series. The inflow was applied at the model cross-section RS 105885.6.

Figure 2.4 presents a comparison of the hourly input flow hydrographs measured for Conestoga River and Pequea Creek. Both USGS gages recorded maxima on 30 October 2012: 16,500 cfs for Conestoga River and 5,000 cfs for Pequea Creek.

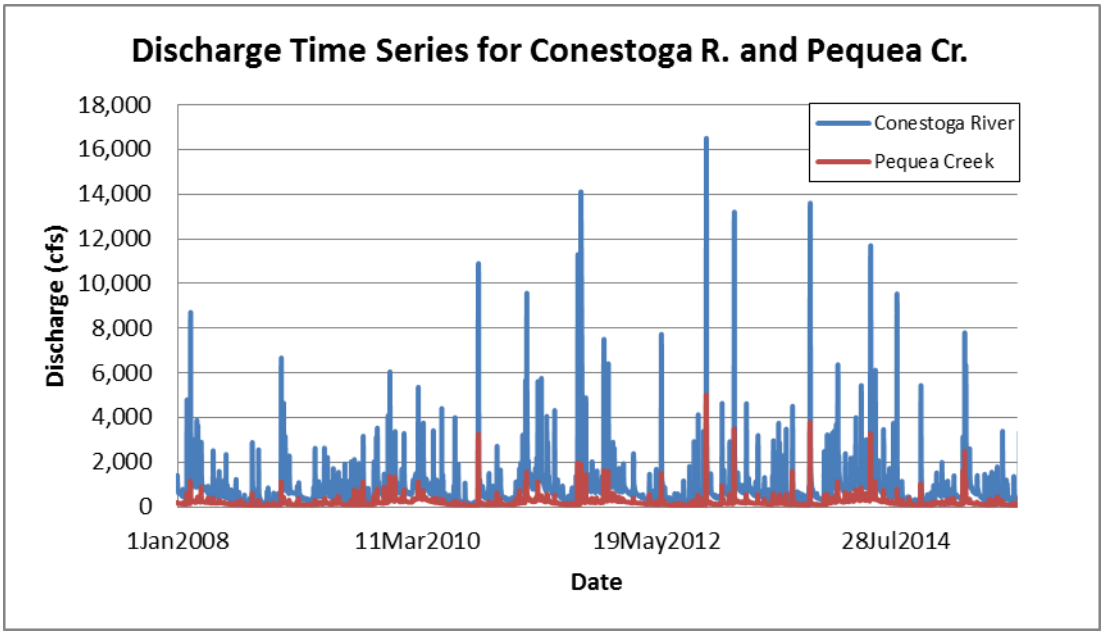

Figure 2.4. Discharge Time Series for Conestoga River and Pequea Creek

2.4 SEDIMENT DATA

In order to simulate erosion, transport, and deposition processes, the HEC-RAS model requires information about bed sediment and additional sediment entering the model with defined inflows at the upstream model boundary and all other inflow locations.

2.4.1 Bed Sediment

Bed particle size gradations for Lake Clarke and Lake Aldred were developed using USGS core data sampled at 35 locations in 1990 and 1991 (Hainly, et al., 1995; Reed & Hoffman, 1996) and provided by the USGS. Langland and Koerkle (2014) used the same coring data to develop bed gradations in their HEC-RAS model and reported good agreement between samples collected in 1990 and 1991 and samples collected in 2000 and described by Edwards (2006). Figure 2.5 shows the locations of the corings.

USGS Coring Locations - Upper Reservoir

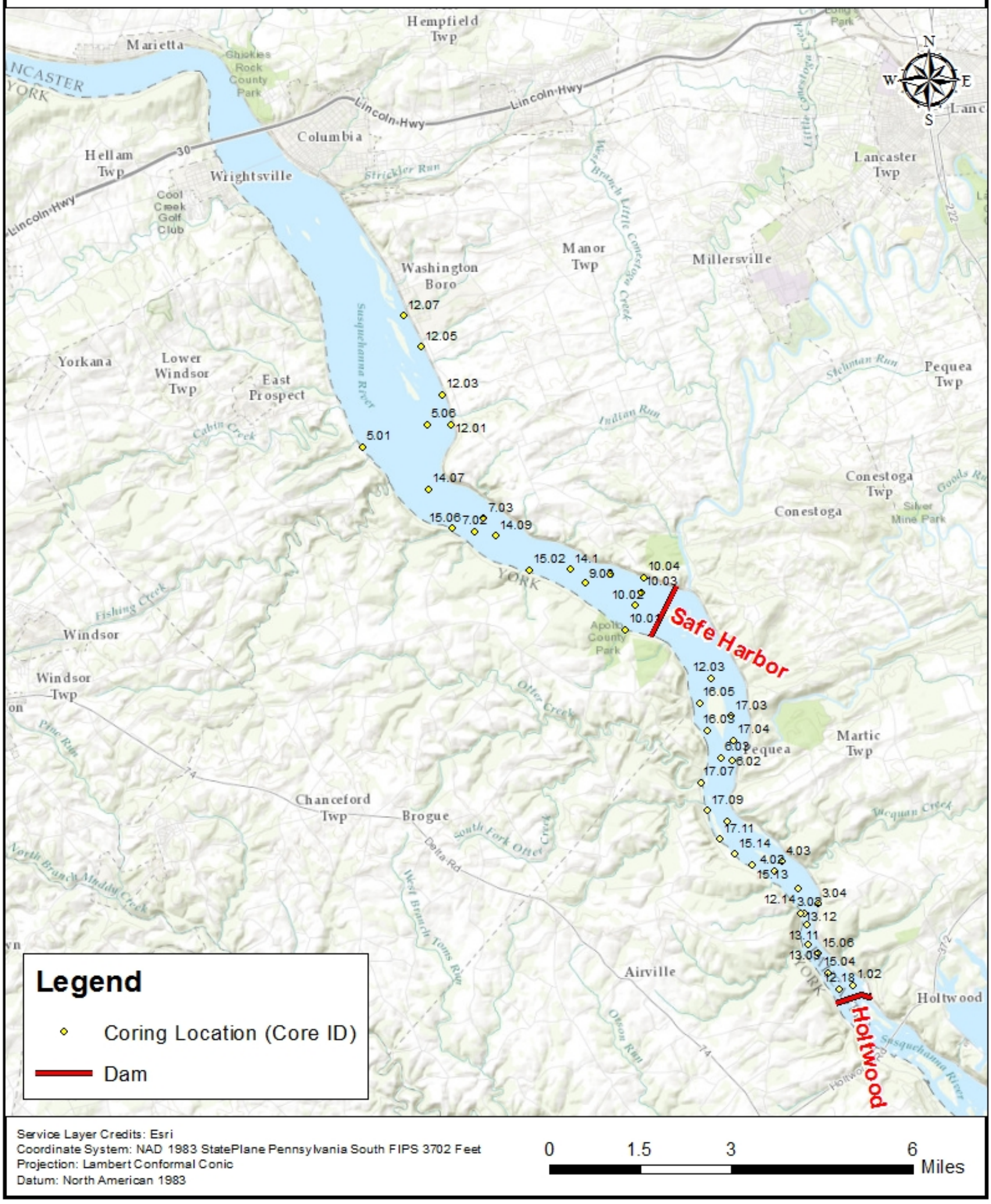

Figure 2.5. Sediment Coring Locations

Ten grouped sediment gradations (A-J) were initially developed to represent bed sediments in Lake Clarke and Lake Aldred, based on trends within sections of each reservoir. For each gradation, particle size distributions from 1 – 5 core samples were averaged and matched with the nearest model cross-sections. Twelve particle size classes ranging from clays (<0.004 millimeters (mm)) to fine gravel (4 – 8 mm) were modeled. Table 2.1 presents the particle size distribution for each grouped bed gradation, along with the corresponding model cross-section(s).

In their model, Langland and Koerkle (2014) defined maximum erodible bed depths in the upper reservoirs as estimates based on Hainly et al. (1995), Reed and Hoffman (1996), and bathymetry data. Those depths varied from approximately 0 to 20 ft. in Lake Clarke, increasing in the downstream direction, and approximately 0 to 10 ft. in Lake Aldred. The same maximum erodible bed depths were assumed as a starting point in the current HEC-RAS model.

The beds in Lake Clarke and Lake Aldred contain significant percentages of silt and clay—cohesive materials—and erosion rates cannot be estimated accurately using standard sand and gravel transport equations. Cohesive forces resist applied shear stresses in beds containing high percentages of fine material, and those forces are highly sensitive to particle size distribution, particle coatings, fine sediment mineralogy, organic content, bulk density, gas content, pore-water chemistry, and biological activity (Scott & Sharp, 2014).

HEC-RAS 5.0 allows users to define cohesive parameters for individual bed gradations, in addition to the previously-available option of assigning global cohesive parameters. This is an important improvement, especially given the high degree of variation in the cohesive properties of the bed sediments of the Lower Susquehanna reservoirs. Langland and Koerkle (2014) noted the inability to model variation in cohesion as an important limitation of their HEC-RAS model. Given the complexity of and variation in cohesive parameters, the HEC-RAS 5.0 manual recommends using direct measurements of particle and mass wasting erosion parameters.

HEC-RAS computes cohesive erosion based on Partheniades (1962), who modeled erosion rates as a function of bed shear. Particle erosion begins as individual particles (or flocs) are removed by bed shear, and the rate of erosion increases almost linearly with increasing shear. At some point, however, higher bed shear can result in the erosion of larger clods, producing an inflection point in the erosion rate. That inflection point, historically, was called the mass wasting threshold, and the term (while ambiguous) was preserved in HEC-RAS for continuity. The erosion rate above the mass wasting threshold is also approximately linear, but typically has a steeper slope (USACE, 2016a). The Sedflume apparatus was used to develop erosion rate data for Conowingo Pond cores by the U.S. Army Corps of Engineers' Engineer Research and Development Center (ERDC) in 2012, and published in Attachment B-2 of the LSRWA (Scott & Sharp, 2014).

Table 2.1. Bed Sediment Gradations.

Grain Class[2]	Size (mm)[3]	Lake Clarke (% Finer)						Lake Aldred (% Finer)			
		A	B	C	D	E	F	G	H	I	J
Clay	0.004	4.5	16.0	36.0	27.7	31.5	22.5	14.0	20.4	2.5	21.3
VF Silt	0.008	5.5	22.5	45.0	40.7	44.5	30.0	18.4	26.8	3.5	29.0
F Silt	0.016	7.5	28.5	55.0	55.7	57.5	40.8	24.2	35.2	5.3	39.3
M Silt	0.031	9.5	37.5	68.0	71.3	70.8	52.3	30.0	45.4	6.8	50.0
C Silt	0.0625	11.5	46.3	83.0	82.0	79.8	59.8	35.0	57.6	9.3	60.3
VF Sand	0.125	14.0	52.3	97.0	87.3	85.0	65.8	41.0	71.2	13.5	70.7
F Sand	0.25	23.0	59.5	99.0	93.3	95.0	82.8	59.6	85.0	29.5	82.0
M Sand	0.5	66.5	80.5	100.0	97.3	99.0	93.5	82.0	94.6	47.8	92.3
C Sand	1	90.0	94.5	100.0	99.7	99.3	99.0	96.4	97.8	60.8	96.0
VC Sand	2	97.0	99.0	100.0	100.0	100.0	99.8	99.4	98.4	69.8	99.0
VF Gravel	4	100.0	100.0				100.0	100.0	99.4	77.0	100.0
F Gravel	8								100.0	100.0	
Corresponding Model Cross-Sections		194127.6, 190454.4, 187225.3, 185640.9, 182695.5, 179019.5, 175574.5, 171968.3, 168449.8, 165660.4, 164038, 160414.1, 157477.8	150842.3, 146692, 145747.9	144467.7, 143399.1	140634, 135766.3	133381.7, 130762.2, 128283.1, 126028.8	124059.3, 122662.5, 121123.2	120389.2, 117482.5, 113547.5, 109917.9, 105885.6	104476.3, 102620.9, 100738.3, 97895.57, 95287.27	93585.01, 90606.45, 88933.34, 87555.42	85854.41, 83655.43, 82742.23, 81117.9, 79676.01

[2] VF = Very Fine, F = Fine, M = Medium, C = Coarse, VC = Very Coarse

[3] Represents maximum particle diameter represented by each particle size class

It was initially hoped that the measured cohesive parameters could be correlated with physical sediment parameters and subsequently applied to coring data collected by others in Lake Aldred and Lake Clarke. Tested sediment parameters included wet bulk density, the D_{10}, D_{50}, and D_{90} particle sizes, the D_{90}/D_{10} ratio, the percentages of sand, silt, and clay, and sample depth below the sediment surface. Unfortunately, no significant correlation was found. Appendix A presents examples of typical correlation coefficient values along with plots of shear threshold, erosion rate, mass wasting threshold and mass wasting rate versus wet bulk density and percentage of clay.

In addition to the lack of strong correlations, the physical sediment properties reported by ERDC differed significantly from those of samples collected by the USGS (analyzed by the USGS and Maryland Geological Survey (MGS)) and AECOM (Zeff, 2016) in Conowingo Pond. In particular, the ERDC samples reportedly contained much smaller percentages of clay than did the AECOM and USGS samples, irrespective of depth (Figure 2.6).

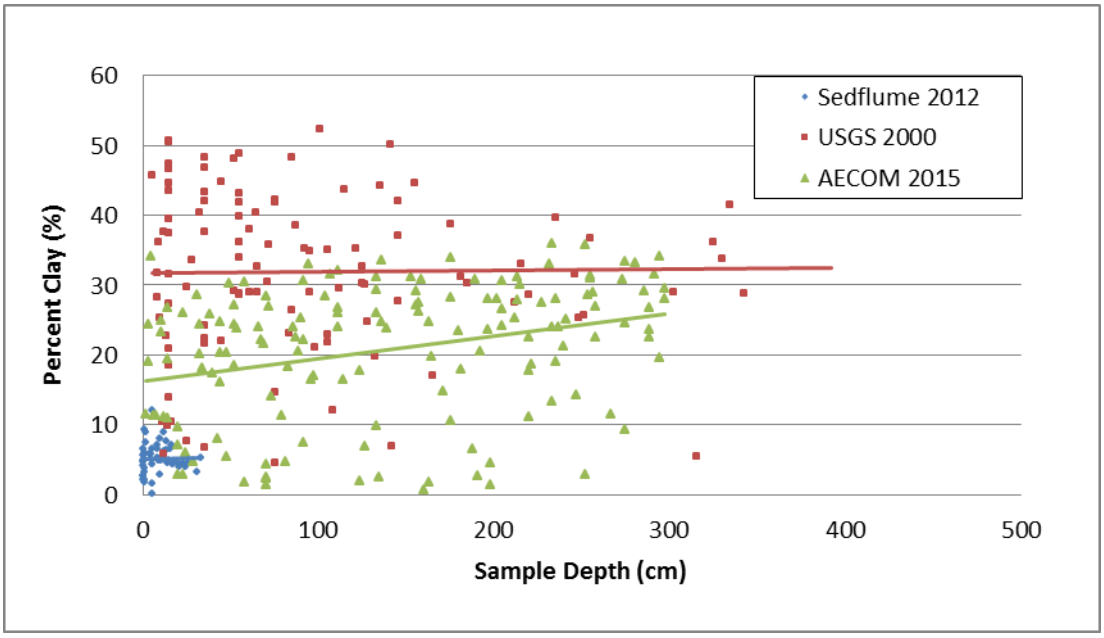

Figure 2.6. Percent Clay vs. Sample Depth for Conowingo: Comparison of USGS, AECOM, and Sedflume Core Data

Based on a review of the particle size analysis methods used by the three groups, it seems likely that the differences in the methods themselves, combined with the reservoirs' unique sediment profiles, were responsible for the apparent disparities in the reported physical properties of the sediments. For example, AECOM, the MGS, and the USGS all used standard, Stokes' law-based methods to analyze silt and clay fractions, while ERDC used laser diffraction. Also, the MGS removed coal and organics from the samples prior to performing the particle size analysis, while the other groups did not. Given that coal and organics are generally lighter than other materials comprising their same size classes, analyses based on Stokes' law and retaining coal and organics probably biased samples towards the finer end of the spectrum (e.g., silt-sized coal was likely measured as clay). The high coal content in the Lower Susquehanna reservoirs (Edwards, 2006) is one of the system's more uncommon features, and complicates reliable comparison of the various particle size analyses.

Rather than attempt to associate the Sedflume measurements taken in Conowingo Pond directly with specific sediment gradations, it was decided to use the percent clay and cohesive parameters as calibration tools, the latter bracketed by the combination of Sedflume-measured values most and least likely to produce scour. Values were converted into U.S. Customary units from the metric units reported by ERDC. Table 2.2 presents the bounding values used in HEC-RAS.

Table 2.2. Bounding Cohesive Soil Parameters.

Parameter	Units	Most Scour Expected		Least Scour Expected	
		Particle Erosion	Mass Wasting	Particle Erosion	Mass Wasting
Threshold	(lb/ft^2)	0.0021	0.0167	0.0334	0.0585
Erosion Rate	($lb/ft^2/hr$)	76.6792	238.1479	7.0781	64.1451

These values also bracket the global cohesive parameters chosen by Langland and Koerkle; while they reported a mass wasting threshold of 0.31 lb/ft^2 (Langland & Koerkle, 2014), a value of 0.031 lb/ft^2 was used in their model.

To develop initial cohesive parameter values, the ERDC cores were grouped by their relative location in the reservoir, as shown in Table 2.3. The percentage of sand generally increases upstream in Conowingo Pond, and comparable sedimentation trends are visible in cores collected in Lake Clarke and Lake Aldred. Cohesive parameters were calculated for each location by averaging the measured values of sub-surface samples from the associated cores. Surface samples were not included, given the thin, low-density, highly-erodible layer noted by ERDC at the sediment-water interface. Mass wasting thresholds and rates for surface samples were not reported by ERDC in Attachment B-2 of the LSRWA (Scott & Sharp, 2014).

Table 2.3. Averaged ERDC Cohesive Parameter Values by Location in Conowingo Pond.

Reservoir Area	ERDC Cores	Particle Erosion Threshold (lb/ft^2)	Particle Erosion Rate ($lb/ft^2/hr$)	Mass Wasting Threshold (lb/ft^2)	Mass Wasting Rate ($lb/ft^2/hr$)
Lower	1, 2, 3	0.0167	40.0565	0.0272	202.2660
Middle	4, 5, 6	0.0250	33.5656	0.0418	77.1707
Upper	9, 10	0.0289	19.8334	0.0585	102.4847

2.4.2 Inflowing Sediment Load

HEC-RAS sediment transport models require information about sediment loading for the upstream boundary and any tributaries. Instantaneous suspended sediment data collected at irregular intervals and corresponding to locations at or very near each USGS gage were downloaded from the USGS and Susquehanna River Basin Commission (SRBC) and combined (USGS, 2016b; SRBC, n.d.). In each case, records lacking complete sediment data were discarded, and records with measured suspended sediment concentration but lacking discharge data were completed using interpolated USGS gaged discharge data when available. All measurements were rounded to the nearest 15-minute interval, and duplicate USGS/SRBC records were compared and one or both deleted. In most cases, duplicate records agreed in their measured values, though it appeared that the USGS records were frequently rounded. In the few cases when differences between synchronous records were irreconcilable, both records were deleted if one was not clearly more reasonable than the other.

Given the infrequency of the sampling, it was not possible to create reliable sediment loading time series, and the measured values were instead used to generate loading-discharge rating curves for each inflow as an HEC-RAS input. Similar to the HEC-6 model developed by Hainly et al. (1995), a positive bias of 2 percent was initially assumed and added to the load as an estimate of unmeasured bedload. Available suspended particle gradation data were also very limited, and gradation rating curves developed for the HEC-6 model using other historic data were adopted and applied to the corresponding discharges. Given the substantial uncertainty in the loading and particle gradation rating curves, the parameters were assigned initial values and later varied during calibration.

In total, 977 unique suspended sediment concentration and accompanying discharge measurements were available for the Susquehanna River near Marietta, PA, measured between 7 October 1986 and 25 April 2015. The maximum discharge with an associated suspended sediment concentration measurement was 449,000 cfs, sampled on 10 September 2011 during Tropical Storm Lee. A rating curve was fit to the sediment loading data, with an R^2 value of 0.86:

$$Q_s = 3 * 10^{-8}(Q + 4000)^{2.35},$$

Where Q_s is sediment loading in tons/day and Q is discharge in cfs.

Table 2.4 presents the sediment loading rating curve and particle gradation curves used as the initial upstream sediment transport boundary condition at Marietta, PA. Note that the value for each grain size class for a given discharge describes the fraction of the total load represented by that size class, rather than the fraction of a sample finer than that particle size.

Table 2.4. Initial Sediment Loading and Particle Size Fractions at Marietta, PA.

Discharge (10^3 cfs)	1	10	36	50	100	200	500	1,000
Total Load (tons/d)	15	169	1,998	4,044	18,869	91,908	769,898	3,888,621
Clay (0.002-0.004 mm)	0.2	0.17	0.15	0.14	0.13	0.12	0.1	0.09
VF Silt (0.004-0.008 mm)	0.18	0.16	0.14	0.14	0.13	0.12	0.1	0.09
F Silt (0.008-0.016 mm)	0.19	0.17	0.15	0.15	0.14	0.13	0.11	0.1
M Silt (0.016-0.032 mm)	0.2	0.17	0.16	0.15	0.14	0.13	0.12	0.1
C Silt (0.032-0.0625 mm)	0.18	0.16	0.14	0.13	0.12	0.12	0.11	0.1
VF Sand (0.0625-0.125 mm)	0.05	0.06	0.08	0.08	0.09	0.09	0.11	0.12
F Sand (0.125-0.25 mm)	0	0.05	0.07	0.09	0.1	0.11	0.11	0.12
M Sand (0.25-0.5 mm)	0	0.04	0.06	0.07	0.08	0.09	0.1	0.1
C Sand (0.5-1 mm)	0	0.02	0.04	0.04	0.05	0.06	0.08	0.09
VC Sand (1-2 mm)	0	0	0.01	0.01	0.02	0.03	0.05	0.05
VF Gravel (2-4 mm)	0	0	0	0	0	0	0.01	0.02
F Gravel (4-8 mm)	0	0	0	0	0	0	0	0.01
M Gravel (8-16 mm)	0	0	0	0	0	0	0	0.01

A total of 1,836 unique suspended sediment records measured between 22 October 1984 and 29 December 2014 were used to develop a rating curve relating sediment loading with discharge for the Conestoga River. A piecewise function of the form shown below was developed to relate sediment loading with discharge, and achieved an R^2 value of 0.779:

$$Q_s = \begin{cases} 1.5 * 10^{-5}(Q-5)^{2.4}, & Q < 1500 \\ 7.3 * 10^{-3}(Q-500)^{1.637}, & Q \geq 1500 \end{cases}$$

Where Q_s is sediment loading in tons/day and Q is discharge in cfs.

Figure 2.7 shows a logarithmic plot of suspended sediment load by discharge, along with the rating curve developed for this study.

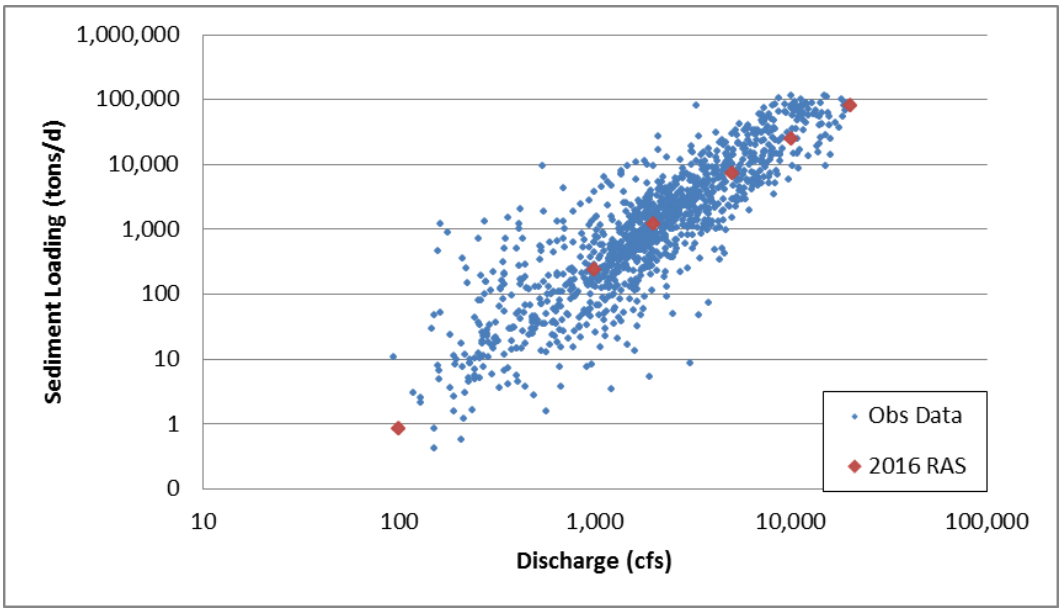

Figure 2.7. Conestoga River Sediment Loading vs. Discharge at Conestoga, PA

Table 2.5 presents the sediment loading rating curve and particle gradation curves used for the Conestoga River lateral inflow.

Table 2.5. Conestoga River Sediment Loading and Particle Size Fractions.

Discharge (cfs)	100	1,000	2,000	5,000	10,000	20,000
Total Load (tons/d)	0.8	235	1,155	6,976	23,706	76,932
Clay (0.002-0.004 mm)	0.32	0.3	0.24	0.22	0.2	0.2
VF Silt (0.004-0.008 mm)	0.2	0.2	0.14	0.14	0.13	0.13
F Silt (0.008-0.016 mm)	0.19	0.19	0.14	0.14	0.13	0.12
M Silt (0.016-0.032 mm)	0.18	0.18	0.14	0.13	0.13	0.12
C Silt (0.032-0.0625 mm)	0.11	0.11	0.13	0.13	0.13	0.13
VF Sand (0.0625-0.125 mm)	0	0.02	0.1	0.11	0.12	0.13
F Sand (0.125-0.25 mm)	0	0	0.08	0.09	0.11	0.12
M Sand (0.25-0.5 mm)	0	0	0.03	0.04	0.05	0.05

A relatively large number (1,960) of suspended sediment measurements were available for Pequea Creek between 11 February 1977 and 15 December 2014, although most samples were taken in the late 1970s. A piecewise function of the

form shown below was developed to relate sediment loading with discharge, and achieved an R^2 value of 0.900:

$$Q_s = \begin{cases} 7.5 * 10^{-6}(Q-15)^{2.93}, & Q < 1500 \\ 14.5(Q-50)^{0.941}, & Q \geq 1500 \end{cases}$$

Where Q_s is sediment loading in tons/d and Q is discharge in cfs.

Figure 2.8 shows a logarithmic plot of suspended sediment load by discharge, along with the rating curve initially developed for this study.

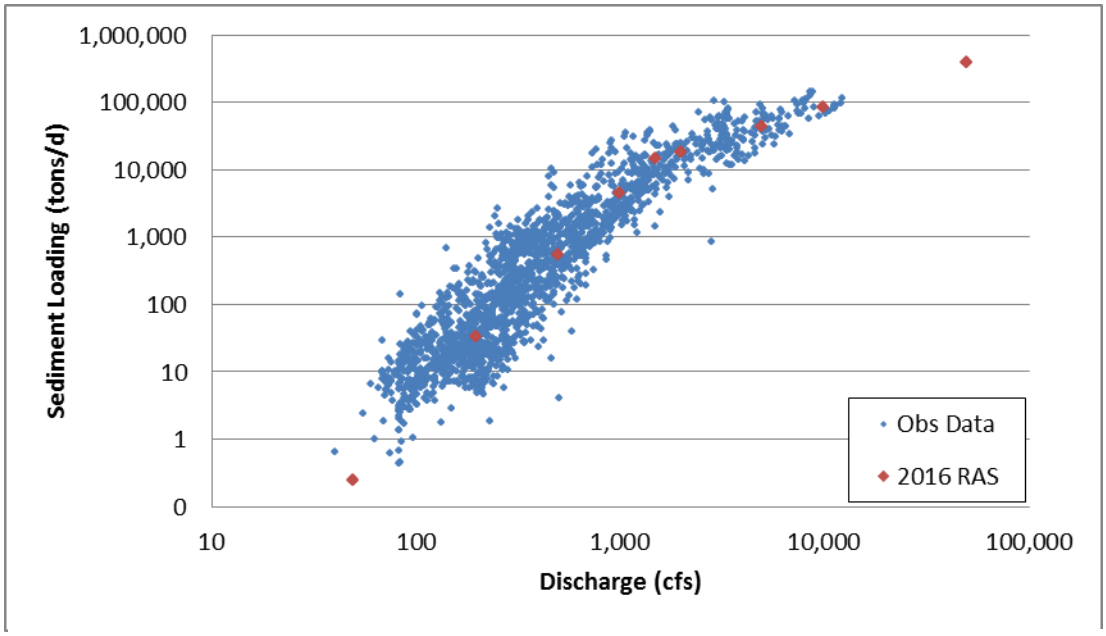

Figure 2.8. Pequea Creek Sediment Loading vs. Discharge at Martic Forge, PA

Table 2.6 presents the sediment loading rating curve and particle size fractions used for the Pequea Creek lateral inflow.

Table 2.6. Pequea Creek Sediment Loading Curve and Particle Size Fractions.

Discharge (cfs)	50	200	500	1,000	1,500	2,000	5,000	10,000	50,000
Total Load (tons/d)	0.25	33	555	4,424	14,731	18,145	43,604	84,120	384,042
Clay (0.002-0.004 mm)	0.32	0.3	0.3	0.24	0.23	0.22	0.2	0.2	0.17
VF Silt (0.004-0.008 mm)	0.2	0.2	0.2	0.14	0.14	0.14	0.13	0.13	0.12
F Silt (0.008-0.016 mm)	0.19	0.19	0.19	0.14	0.14	0.14	0.13	0.12	0.12
M Silt (0.016-0.032 mm)	0.18	0.18	0.18	0.14	0.14	0.13	0.13	0.12	0.12
C Silt (0.032-0.0625 mm)	0.11	0.11	0.11	0.13	0.13	0.13	0.13	0.13	0.13
VF Sand (0.0625-0.125 mm)	0	0.02	0.02	0.1	0.1	0.11	0.12	0.13	0.14
F Sand (0.125-0.25 mm)	0	0	0	0.08	0.09	0.09	0.11	0.12	0.13
M Sand (0.25-0.5 mm)	0	0	0	0.03	0.03	0.04	0.05	0.05	0.06
C Sand (0.5-1 mm)	0	0	0	0	0	0	0	0	0.01

2.4.3 Transport Function and Sediment Parameters

Initially, the Laursen (Copeland) transport function was selected for the Lower Susquehanna River, based on the method's established performance in predominately silt-bedded rivers. The Thomas (Exner 5) sorting method was applied, along with the Report 12 fall velocity method.

HEC-RAS 5.0 features a number of options designed to improve predictions of spatially-variable sediment transport within a one-dimensional modeling framework. The reservoir deposition option, which deposits more material in deeper parts of the cross-section rather than depositing a veneer of equal thickness across all wetted areas, was applied for the model.

Unfortunately, while HEC-RAS 5.0 allows users to define sample-specific cohesive parameters for bed gradations, other sediment parameters such as specific gravity and dry unit weights are applied globally. While some bed and inflowing sediments may be slightly lighter due to the presence of coal, the default values for specific gravity and unit weight by size class were applied (Table 2.7). Note that the modeled bed and inflowing sediment gradations are mixtures of size classes. Therefore, the dry unit weights will be composited values and reflect the proportion of material in the three global classes in the table.

Table 2.7. Global Values for Specific Gravity and Unit Weights.

Specific Gravity (dimensionless)	Unit Weight Sand (lb/ft^3)	Unit Weight Silt (lb/ft^3)	Unit Weight Clay (lb/ft^3)
2.65	93	65	30

Sediment was routed using the continuity method, and a single mobile bed channel was used for all cross-sections (i.e., the braided channel feature in version 5.0 was not employed).

2.5 TEMPERATURE DATA

HEC-RAS sediment transport modeling requires users to enter a time series of water temperature data, which is used to calculate fall velocities in sediment transport computations. A fifth-order polynomial was fit to 205 water temperature measurements taken between 2008 and 2014 at the Marietta, PA streamgage (USGS 01576000) and used to relate temperature with the day of the year. A discontinuity between November 15 and December 31 was removed, and the missing days were interpolated linearly in HEC-RAS. A temperature time series was created for the simulation period, and observed data were used when available.

All temperatures were measured between 6:30 AM and 6:30 PM, with the average measurement taken at 12:10 PM. A separate, 15-minute USGS temperature time series available from May to September 2015 suggests a maximum diurnal flux of <3°C, with small fluxes in most summer months. Given the assumed negligible impact, temperatures were not corrected for diurnal fluxes.

Figure 2.9 presents the fifth-order polynomial and its fit to the observed temperature data, while Figure 2.10 shows the hybrid time series consisting of both observed and generated daily temperatures used as input to the HEC-RAS model.

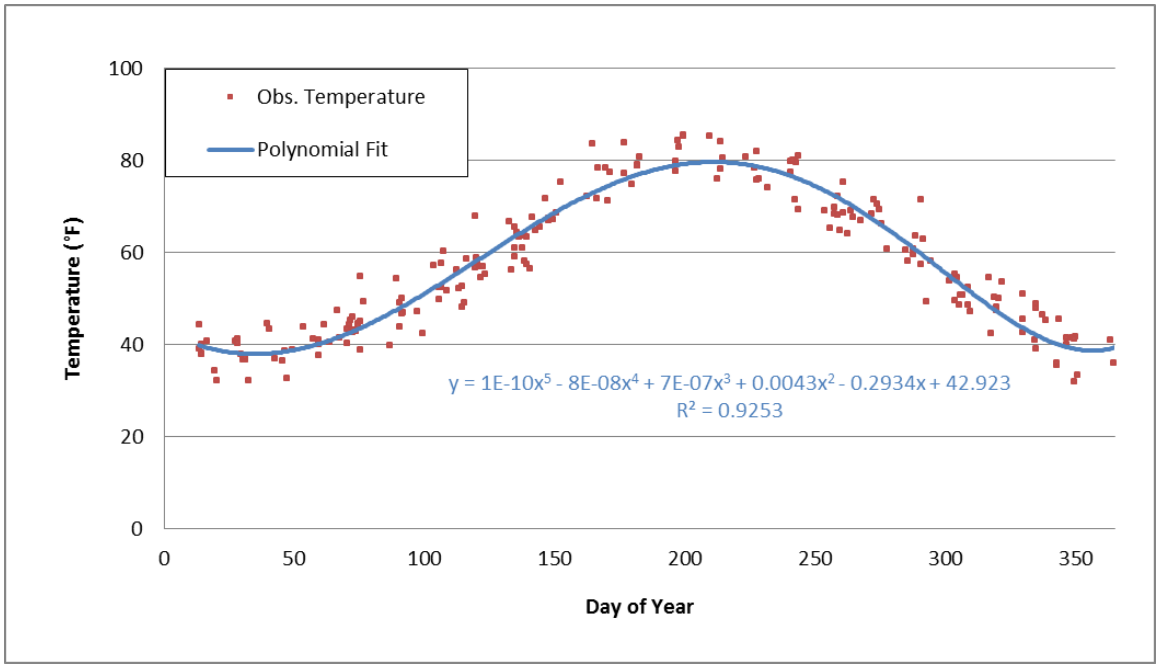

Figure 2.9. Water Temperature by Day of Year

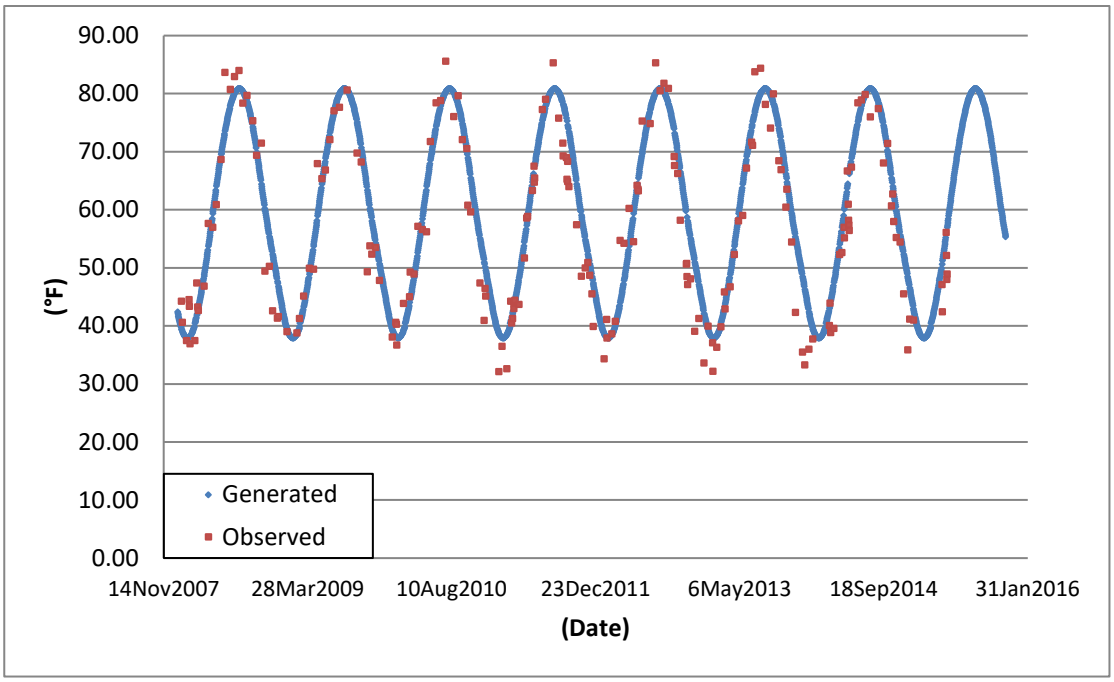

Figure 2.10. Hybrid Water Temperature Time Series

2.6 DAM OPERATIONS

Safe Harbor and Holtwood Dams are operated by the SHWPC and Brookfield Renewable Energy Partners, respectively. While some information about normal pool levels and structure dimensions is available online, details of day-to-day dam operations are largely unavailable. Langland and Koerkle (2014) modeled Safe Harbor Dam using a time series of gate openings designed to maintain a target pool elevation, and modeled Holtwood Dam as a weir.

Rather than attempt to explicitly mimic hour-to-hour or day-to-day gate operations, rating curves were developed for both dams for the current model, based on available information. According to the SHWPC (Safe Harbor Water Power Corporation, n.d.), the normal pool elevation for Safe Harbor is 227.2 ft., corresponding to the NGVD29 vertical datum. The powerhouse has a capacity of 113,000 cfs, while the flood gates have a capacity of 1,120,000 cfs. At no point in the simulation period does the river's discharge exceed Safe Harbor's gate capacity, and while water surface elevations in the reservoir vary at flows below the powerhouse capacity (based on peaking operations), the water surface elevation is maintained within a range of approximately 224 to 228 ft. Figure 2.11 shows the rating curve implemented as an internal boundary at Safe Harbor, and Figure 2.12 shows the range of water surface elevations upstream of the dam over the simulation period.

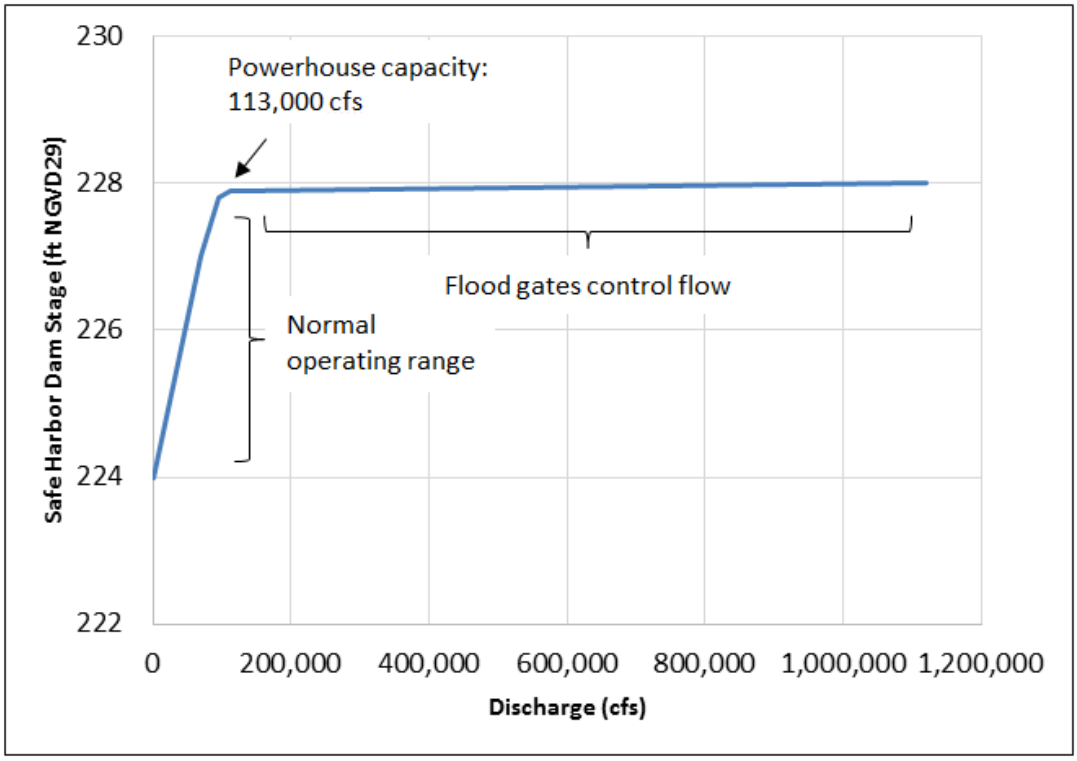

Figure 2.11. Safe Harbor Dam Interior Boundary Rating Curve

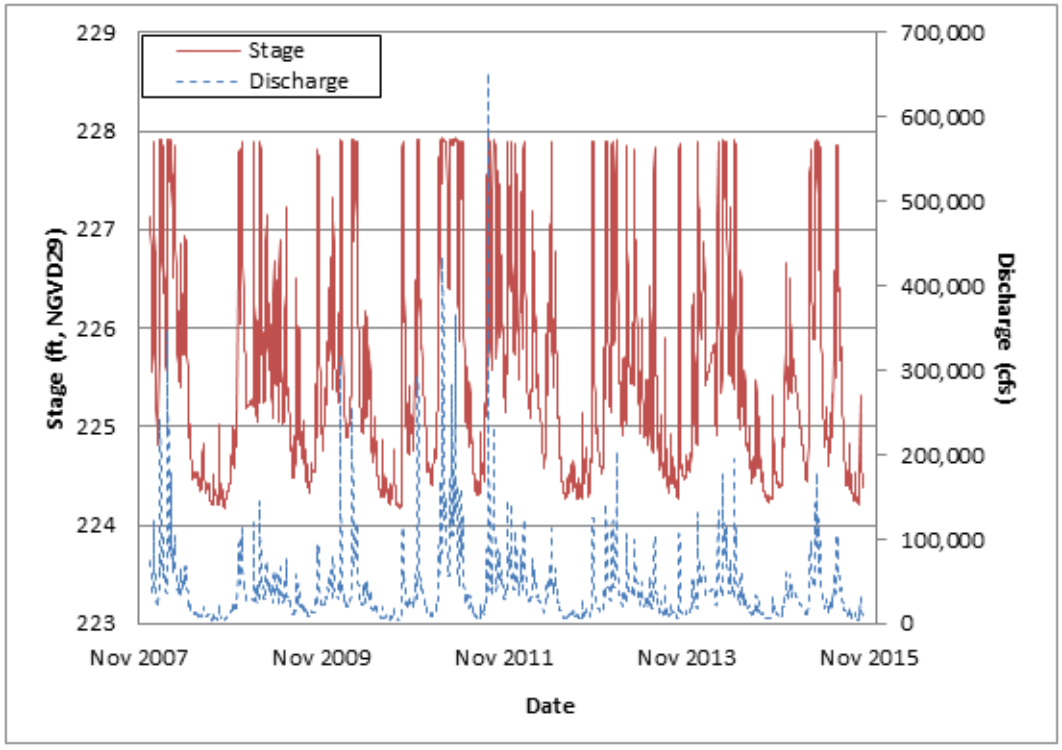

Figure 2.12. Simulated Stage and Discharge Series at Safe Harbor Dam

Holtwood Dam has relatively limited control of the river, and aside from its power production units and a 4.75-foot inflatable rubber dam, the structure essentially functions as a weir. The published normal pool elevation—that is, the elevation at which the rubber dam is crested and the dam begins to spill—is 169.75 ft. (Safe Harbor Water Power Corporation, n.d.). The vertical datum is not listed on the website, and it was discovered that the value is actually referenced to a local datum at Holtwood (Sullivan, 2016a). When converted to the NGVD29 datum, the target pool elevation is 170.52 ft. A composite rating curve was developed to represent stage vs. flow at the downstream boundary. Stage heights ranged linearly from 165.77 ft. to 170.52 ft. for flows below 61,460 cfs, reflecting assumed operation of the flashboards/rubber dam within the operating capacity of the powerhouse. A weir coefficient of 3.7 was assumed for the flashboards/rubber dam, and those were assumed to fail gradually between 2 and 4 feet above the flashboard height. The powerhouse was assumed to gradually shut down between a total flow of 350,000 and 375,000 cfs, at which point the dam functioned as a weir with an assumed coefficient of 4.06. Figure 2.13 shows the shape of the rating curve applied as the downstream boundary, and Figure 2.14 shows the range of water surface elevations upstream of the dam over the simulation period.

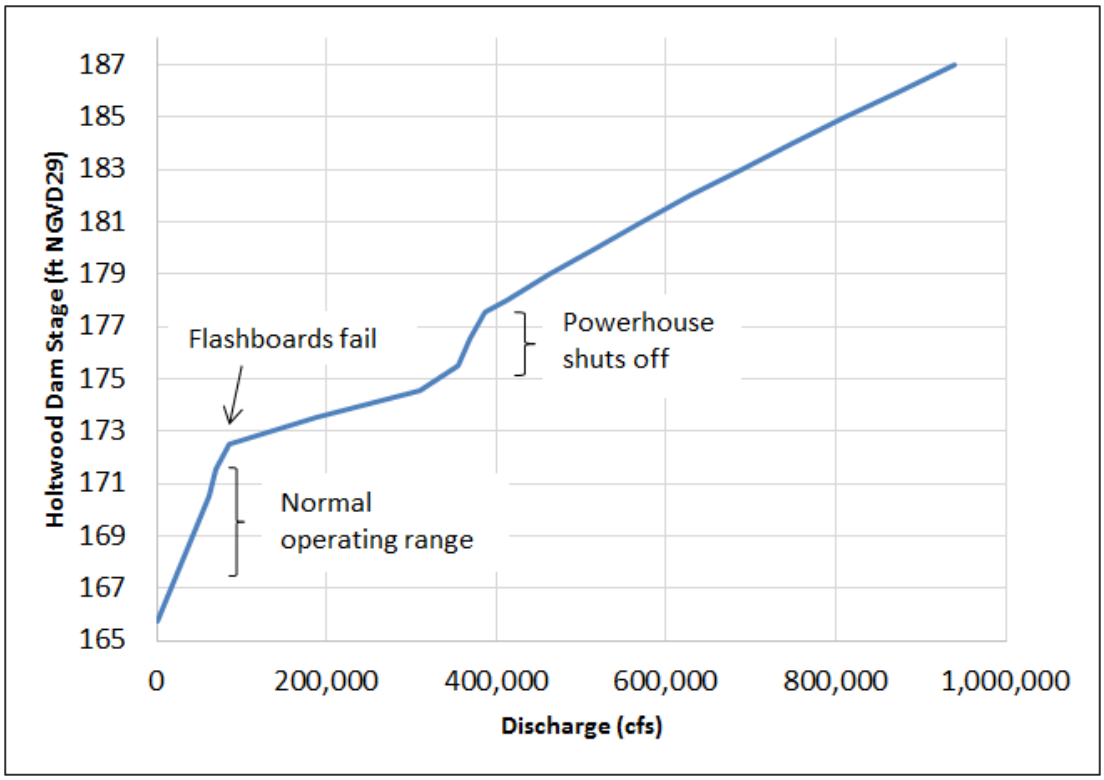

Figure 2.13. Holtwood Dam Boundary Rating Curve

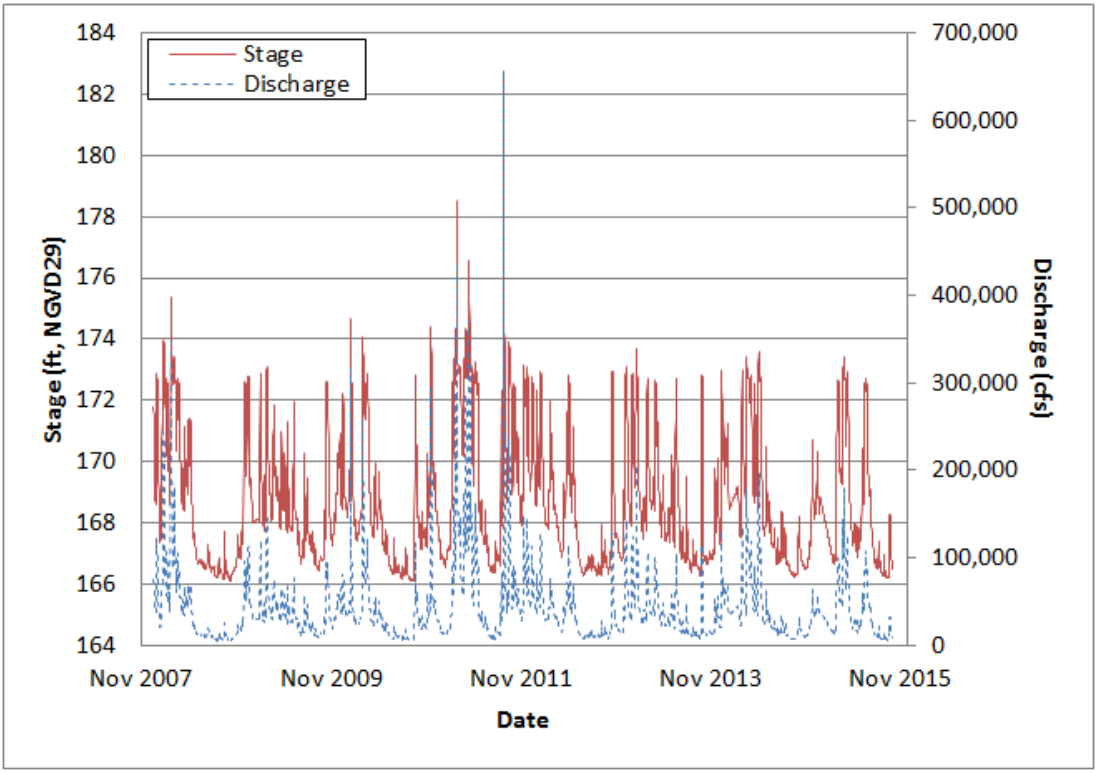

Figure 2.14. Simulated Stage and Discharge Series at Holtwood Dam

3 MODEL CALIBRATION

The modeling effort was designed with a three-phase calibration-verification process. First, the hydraulics of the fixed-bed unsteady flow model were calibrated for the simulation period 1 January 2008 – 30 August 2013. Next, the unsteady sediment transport model was run and calibrated to bed volume change from the same period. Finally, the sediment transport model was verified using calculated bed volume change for 1 January 2008 – 15 October 2015.

3.1 FIXED-BED CALIBRATION

One challenge to the calibration of a fixed-bed hydraulic model for the Lower Susquehanna River system was the lack of historic, inter-system stage and flow data with which to compare the modeled results. The three hydraulic structures located between the USGS streamgage at Marietta, PA and the USGS streamgage immediately downstream of the powerhouse at Conowingo Dam control the flows to varying degrees, yet no gaged data are available to confirm modeled results between the dams. However, the gage at Marietta does provide a useful check on the upstream end of the unsteady, fixed-bed model, through a comparison of over 120 instantaneous stage measurements made during the calibration period with the water surface elevation predicted by the model.

Despite the challenges of limited input data, the fixed-bed model performed well with very little calibration.

After altering the upstream boundary to match the gage's location and adjusting the Manning's *n* values by season and discharge, modeled water surface elevations matched observed values to within an average of approximately ±0.34 ft. over the full range of discharges during the calibration period. Error was generally one of timing rather than magnitude, and was likely attributable to the combination of a relatively-coarse 12-hour hydrograph output interval and the steep hydrograph slopes. A visual comparison of the observed and modeled water surface elevations shows an offset of less than 12 hours between observed and modeled stages for almost all large events. Figure 3.1 presents a comparison of the observed and modeled stages over the full hydraulic calibration period, while Figure 3.2 shows the apparent timing offset visible during storm events in January and February 2010.

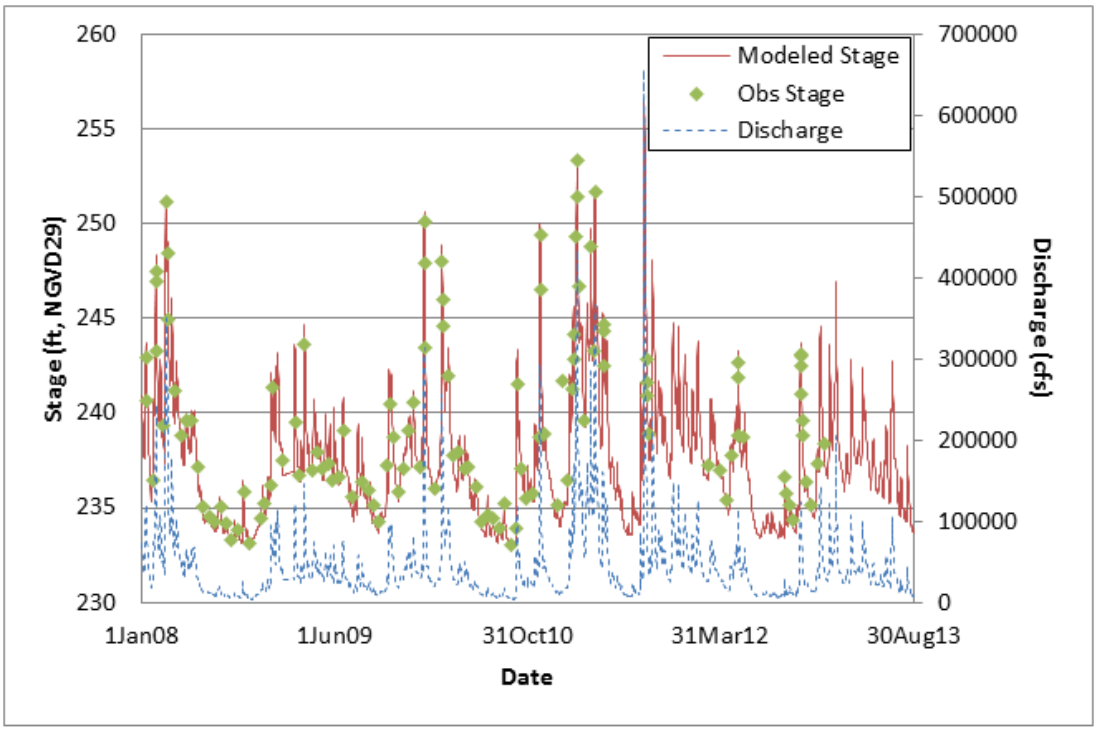

Figure 3.1. Observed and Modeled Stage Elevation at Marietta, PA: Calibration Period

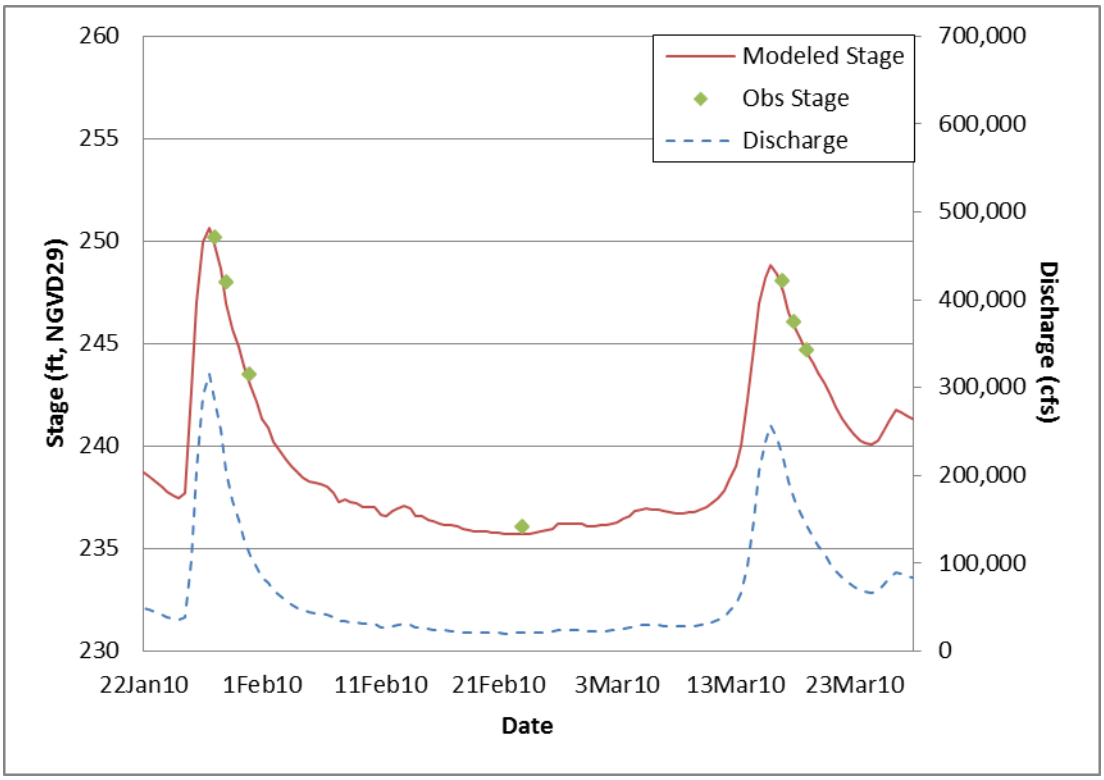

Figure 3.2. Observed and Modeled Stage Elevation at Marietta, PA: Spring 2010

3.2 SEDIMENT TRANSPORT CALIBRATION

As with the hydraulic calibration, the lack of historic gaged data between the dams presents a major challenge to calibrating sediment transport models within the Lower Susquehanna reservoir system. While a comparison of suspended sediment concentrations upstream of Lake Clarke and downstream of Conowingo Reservoir permits some evaluation of the system as a whole, it is difficult to parse deposition and scour processes within the three reservoirs. In order to perform the calibration and verification, a measure of change was developed, a sensitivity analysis was performed, and the model parameters were systematically altered within reasonable ranges to approach the desired results.

3.2.1 Sediment Volume Change

In lieu of inter-system gaged sediment transport data, changes in bed volume over time provided an alternate source of calibration data for this study. While the temporal resolution of the calibration was limited to the frequency of historic bathymetric surveys, the relatively high spatial resolution of the cross-sections within the reservoirs provided some insight into the bed regions more prone to deposition and/or scour.

Several methods for computing volume change were evaluated, including an average end-area method, based on HEC-RAS geometry files created for each bathymetric survey dataset of interest, and GIS-based terrain development and analysis. The volume change calculations were very sensitive to both the method and number of surveyed cross-sections used, and calculated volume changes varied significantly between methods. Ultimately, Gomez and Sullivan applied a GIS-based method to calculate volume change, and provided the results to WEST for use in model calibration and verification.

The cross-sections from Langland and Koerkle's 2014 HEC-RAS model were assumed for analysis purposes to represent the 2008 bathymetry collected by the USGS. In reality, they were developed using a combination of 1996 and 2008 USGS survey data, LiDAR data, data from a historical flood insurance study, and hand-interpolated cross-sections (Langland & Koerkle, 2014; Sullivan, 2016a; MDNR, 2014). In many cases, the georeferenced cross-sections in the model did not align well with the transects reported in Figure 5 and 7 in Langland's 2009 report (Langland, 2009). Gomez and Sullivan's 2013 and 2015 survey transects were aligned to the georeferenced cross-sections published in Langland's 2009 report, as the 2013 survey was planned and initiated prior to publication of the 2014 model and actual survey data. The 2015 survey repeated data collection along the same transects to allow for direct comparisons of changes in bed volume from year to year. In addition to collecting data along what were believed to be the same cross-section transects as the 2008 USGS survey, Gomez and Sullivan's surveys also included supplemental cross-sections and longitudinal transects to increase the survey density.

In order to minimize apparent bed volume changes due to differences in the number and locations of cross-sections, rather than actual volume change, a set of common cross-sections was selected based on those with good spatial agreement between the USGS survey and model datasets and the Gomez and Sullivan bathymetry data. The common cross-sections were then used to develop terrains in ArcGIS to allow for direct comparisons of bed volume changes from year to year. The cross-sections which were not spatially-aligned to a reasonable degree were discarded, as were extra transects in the Gomez and Sullivan survey data. The survey points from each dataset were normalized to the common cross-section lines.

Figure 3.3 and Figure 3.4 present a comparison of the survey transects published in Langland (2009), the cross-sections surveyed in 2013 and 2015 by Gomez and Sullivan, and the cross-sections used in the Langland and Koerkle HEC-RAS model (2014). Figure 3.5 and Figure 3.6 show the common cross-sections used in the volume change calculations and the associated USGS/Gomez and Sullivan-collected survey points, prior to normalization.

Bathymetric terrains were created for each survey year (2008, 2013, and 2015), and volume changes below the normal pool elevations were calculated using the Cut/Fill tool in ArcMap for the 2008-2013 and 2013-2015 periods.

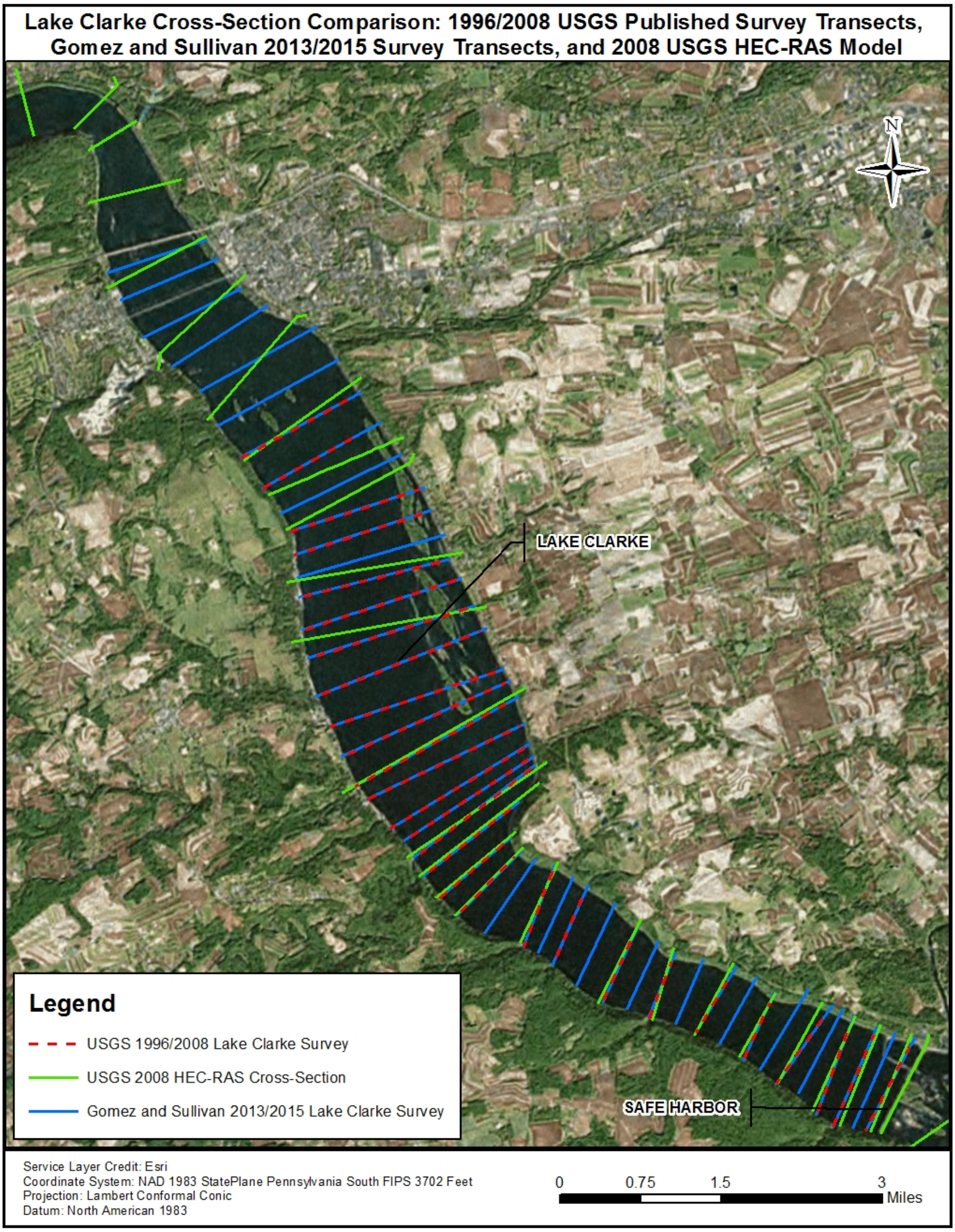

Figure 3.3. Comparison of Published 1996 and 2008 USGS Survey Transects (Langland 2009), USGS HEC-RAS Model Cross-Sections (Langland and Koerkle 2014), and 2013/15 Gomez and Sullivan Survey Cross-Sections

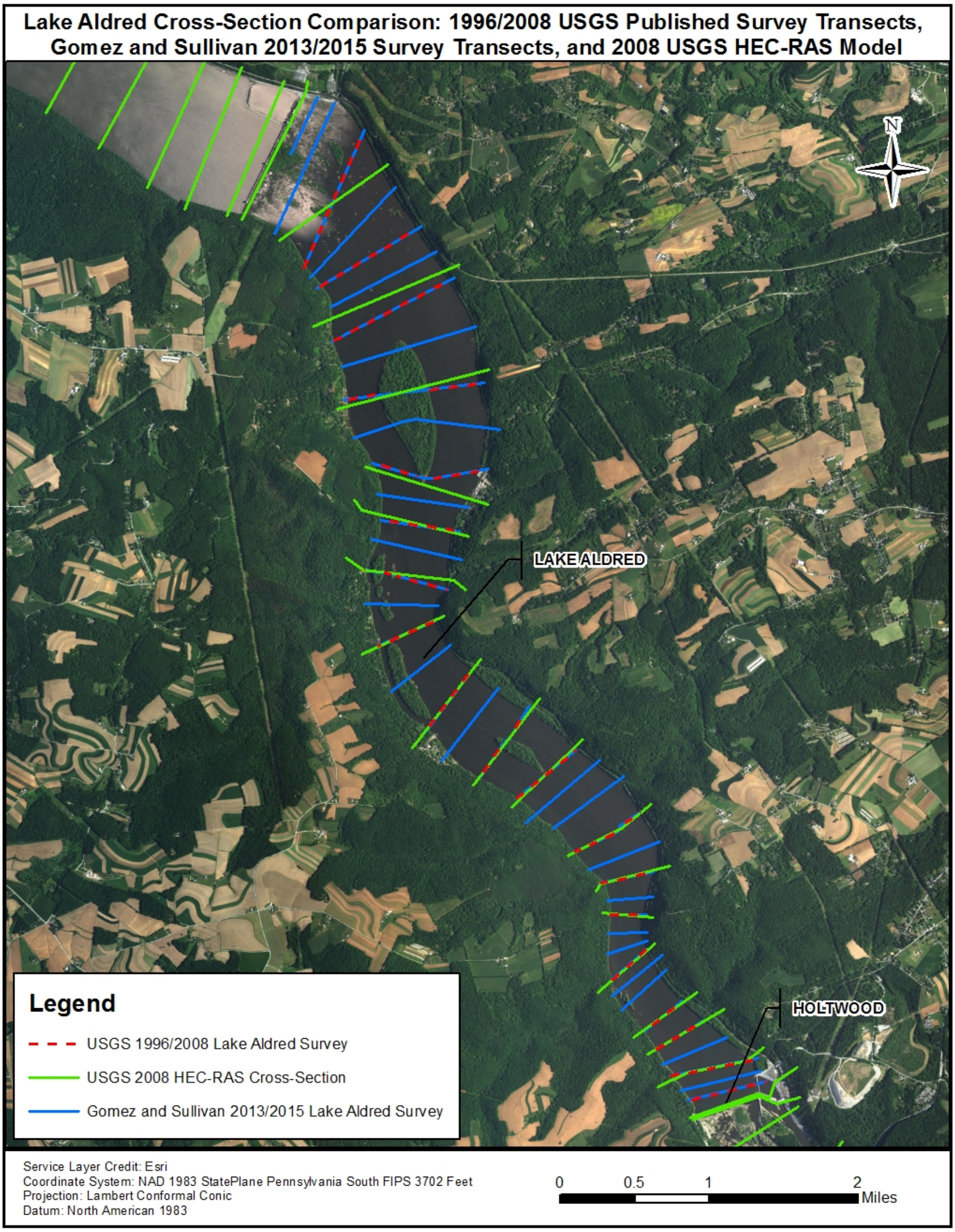

Figure 3.4 (Cont'd). Comparison of Published 1996 and 2008 USGS Survey Transects (Langland 2009), USGS HEC-RAS Model Cross-Sections (Langland and Koerkle 2014), and 2013/15 Gomez and Sullivan Survey Cross-Sections

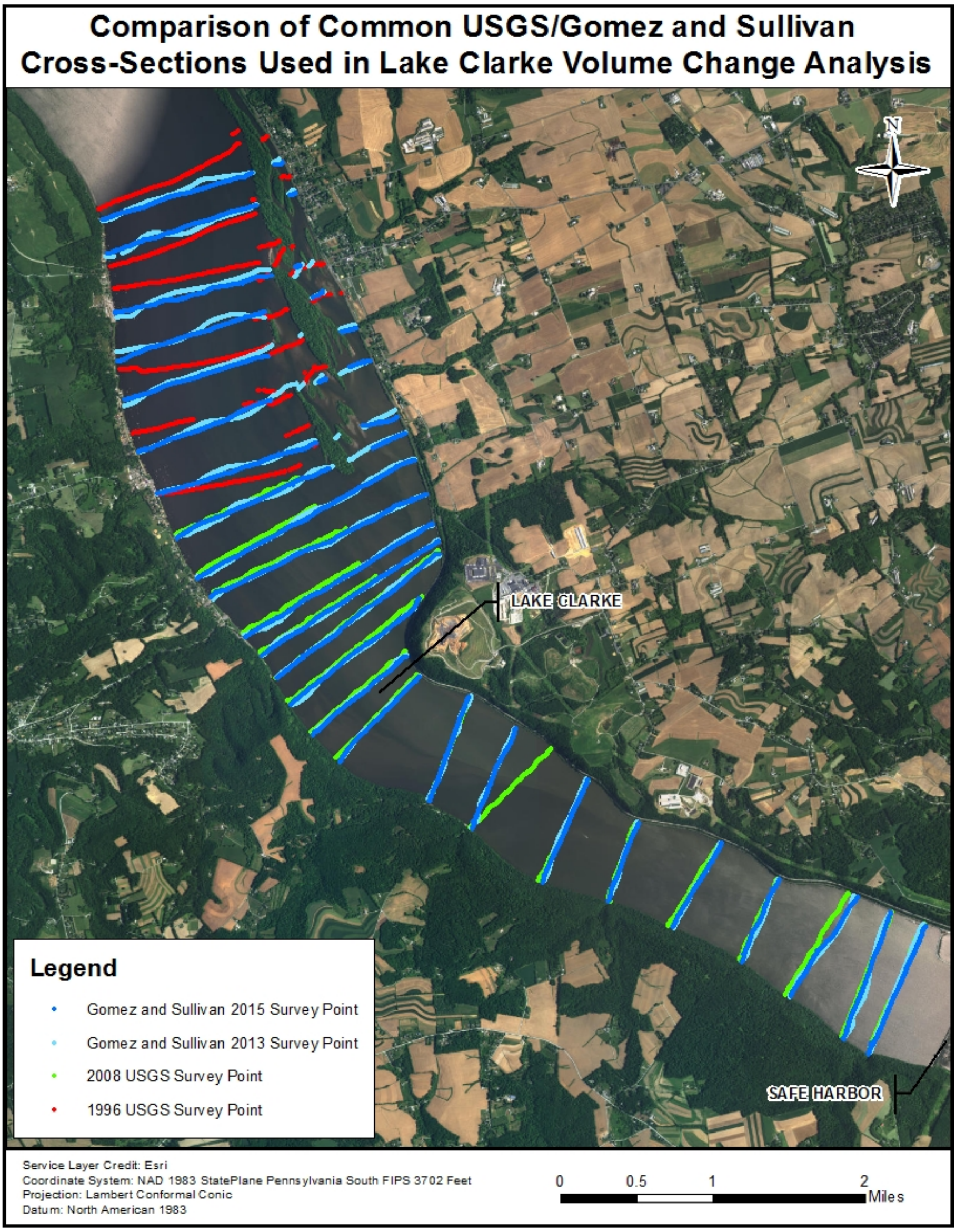

Figure 3.5. Comparison of Common Cross-Sections Used in Volume Change Analysis With Associated USGS/GSE-Collected Survey Points, Prior to Normalization

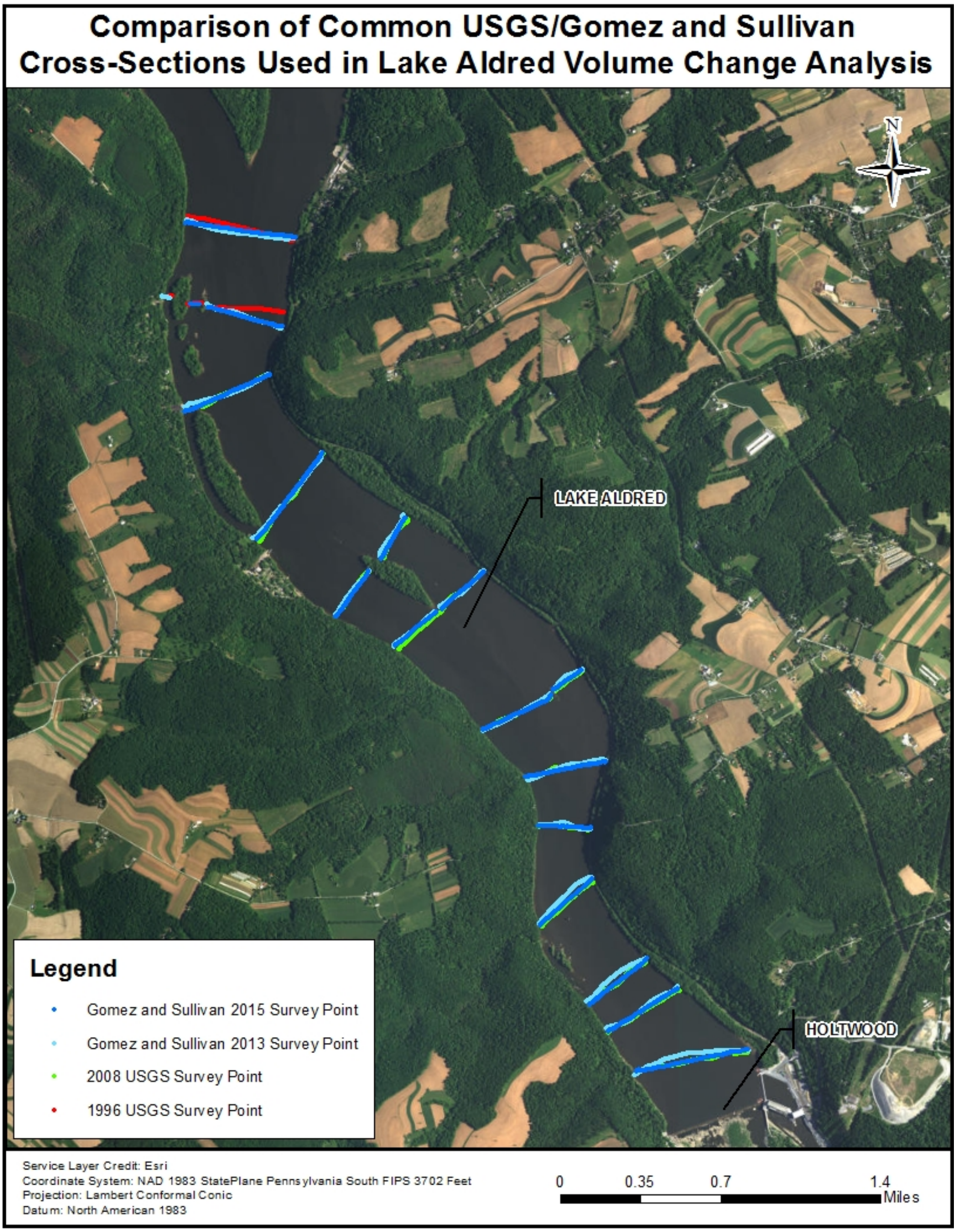

Figure 3.6 (Cont'd). Comparison of Common Cross-Sections Used in Volume Change Analysis With Associated USGS/GSE-Collected Survey Points, Prior to Normalization

The limitations of the volume change calculation method were more pronounced in some areas than in others. For example, the 2013-2015 volume change in Lake Aldred calculated using a) all of the GSE cross-sections or b) only those which corresponded to the USGS cross-section locations varied significantly, primarily due to the process of normalizing to a relatively small number of cross-sections in the latter. Lake Aldred is narrow and deep, with many steep-walled areas, and normalizing a cross-section by as little as 50-100 feet produced large changes. This issue was most pronounced for the upstream third of the 2008 terrains for each reservoir, which was comprised of the 1996 USGS survey data. The 1996 raw survey points were frequently oriented several hundred feet from the final, normalized cross-sections used by Langland and Koerkle (2014) to create the HEC-RAS model geometry.

As a result of the greater uncertainty in the upstream areas of each reservoir, the lakes were each split into a number of sub-areas, and the sub-areas with the greatest degrees of certainty (five in Lake Clarke, four in Lake Aldred) were selected for the calibration. Figure 3.7 shows the sub-areas used in the analysis, along with the orientation of the HEC-RAS cross-sections for reference. Note that the sub-area numbering decreases in the downstream direction in Lake Clarke, and increases in the downstream direction in Lake Aldred. Also, note that the colors are only intended to distinguish between the sub-areas, and do not provide additional information.

All volume change calculation methods indicated net deposition over both time periods for Lake Clarke and little net change for Lake Aldred. Calculated changes were relatively small in terms of the system as a whole. For example, an error of ±0.15 feet (the assumed accuracy of the survey equipment in Lake Clarke based on depth), would produce a difference of almost 44,000,000 ft^3 (~1,000 acre-feet) when applied over the entire reservoir bed. For the deeper Lake Aldred, the accuracy of the survey equipment was assumed to be ±0.5 feet—an error which would, if consistently biased over the whole reservoir, produce a difference of over 46,000,000 ft^3 (~1,060 acre-feet). As a result of the uncertainty in the volume change calculations, a range was calculated for each sub-area based on the assumed accuracy of the survey equipment. Table 3.1 presents the ranges for each of the sub-areas used in the model calibration and verification, based on the GIS analysis method.

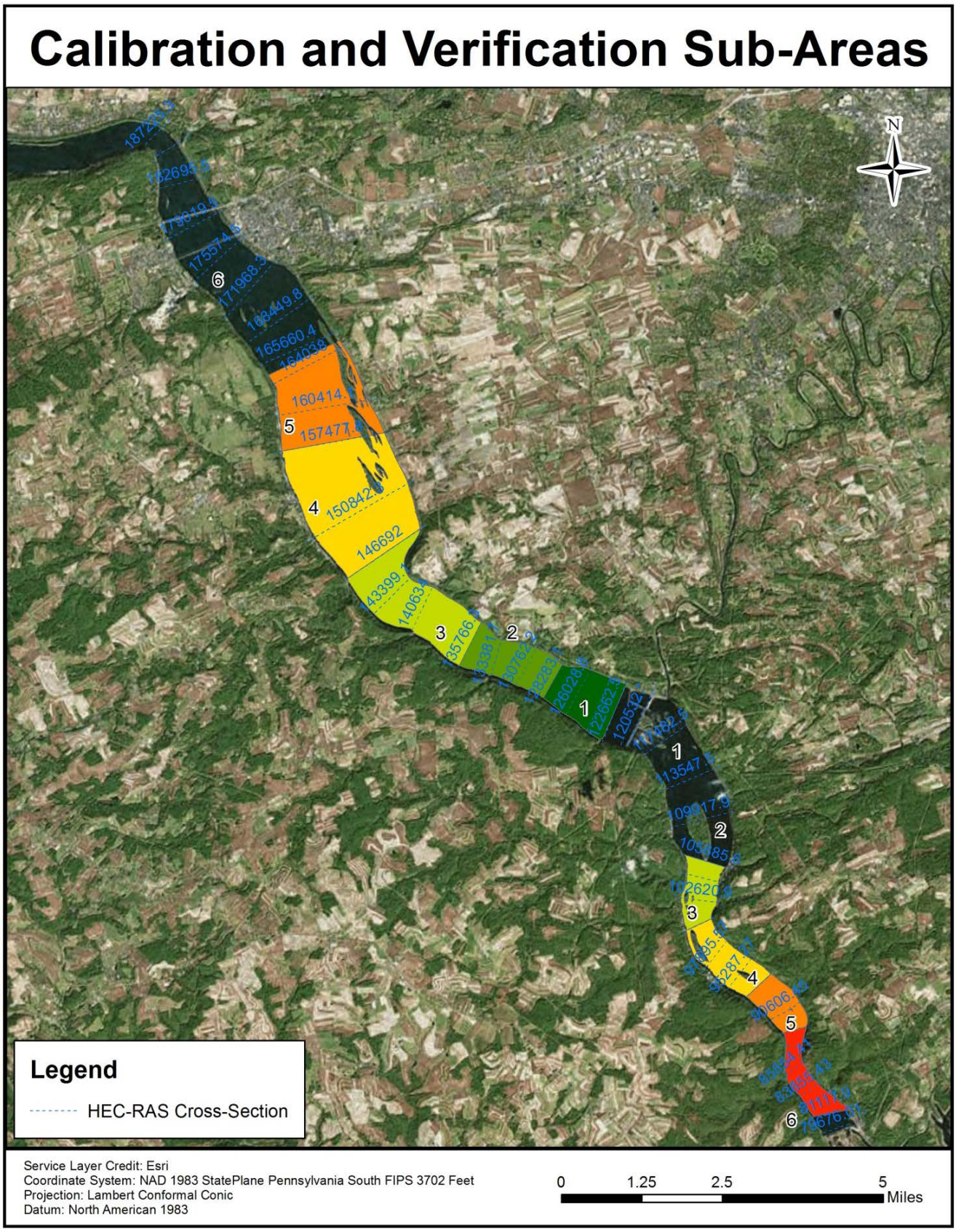

Figure 3.7. Reservoir Sub-Areas Used in Calibration and Verification (Non-Colored Sub-Areas Not Used in Analysis)

Table 3.1. Observed Volume Changes by Sub-Area.

		Observed Volume Change (ft^3)			
		2008-2013		2013-2015	
		Low Range	High Range	Low Range	High Range
Lake Clarke	Sub-area 5	-9,501,201	4,878,069	-2,328,329	12,050,941
	Sub-area 4	64,027,132	88,688,002	10,413,004	35,073,874
	Sub-area 3	43,067,414	57,118,004	21,348,085	35,398,675
	Sub-area 2	20,651,174	28,159,094	11,924,155	19,432,075
	Sub-area 1	27,568,843	34,468,633	1,824,112	8,723,902
	Total	145,813,362	213,311,802	43,181,027	110,679,467
Lake Aldred	Sub-area 3	-15,483,159	-1,678,359	-8,769,671	5,035,129
	Sub-area 4	-15,290,579	2,606,521	-5,927,657	11,969,443
	Sub-area 5	6,838,284	19,855,684	-5,196,278	7,821,122
	Sub-area 6	8,092,159	22,145,659	-14,248,858	-195,358
	Total	-15,843,294	42,929,506	-34,142,463	24,630,337

3.2.2 Sensitivity Analysis

Prior to calibration, the model's sensitivity to various input parameters was tested to identify the most promising parameters to use for calibration. Given the high degree of uncertainty in many of the model's boundary conditions, a large number of parameters was evaluated, including changes to Manning's *n* values, hydraulic controls, sediment loading and gradations, mobile bed limits, bed gradations and cohesion, global sediment parameters, transport functions, bed sorting and fall velocity methods, and other inputs.

Of the various inputs, Manning's *n*, the depth of the erodible bed sediment, the percentage of bed clay, bed cohesive parameters, sediment inflow loading and composition, and the transport function were recognized as strong candidates for calibration parameters given the sensitivity of model results to their values and the uncertainty in the input data.

In addition to the calibration parameters, the sensitivity analysis also helped identify two sections of the model where initial simulated results diverged most from observed bed volume change. First, Lake Clarke's sub-area 5 is characterized by a very wide, flat channel with areas of adverse bed slope and a network of ineffective side channels—features generally associated with depositional zones—while very little deposition or net scour was actually observed between surveys. Second, observed volume change in Lake Aldred generally increased in the downstream direction between 2008 and 2013, with the most deposition observed in sub-area 6.

The initial simulated results revealed the opposite trend—decreasing deposition in the downstream direction—similar to the trend seen during the 2013-2015 period. These two reaches (Lake Clarke's sub-area 5 and Lake Aldred's sub-areas 3-6) emerged from the sensitivity analysis as the primary challenges to matching reservoir-wide trends in model calibration.

3.2.3 Model Calibration

Calibration was performed by running the model from 1 January 2008 through 30 August 2013—a period characterized by several large events, including Tropical Storm Lee—and systematically varying parameters to produce results approaching the observed bed volume changes for the same period.

To begin, the Toffaleti transport function was applied to the model in place of the Laursen (Copeland) method. While the Toffaleti transport function was originally developed for rivers with slightly coarser mean bed particle size (very fine sand or coarser; about half of the model cross-section bed gradations met this criterion), it has been used successfully on rivers of similar size. Figure 3.8 shows the transport function's effect on bed volume change. Notably, the function resulted in decreased local extremes, reducing excessive modeled deposition in Lake Clarke's sub-area 5 with little effect on net volume change overall.

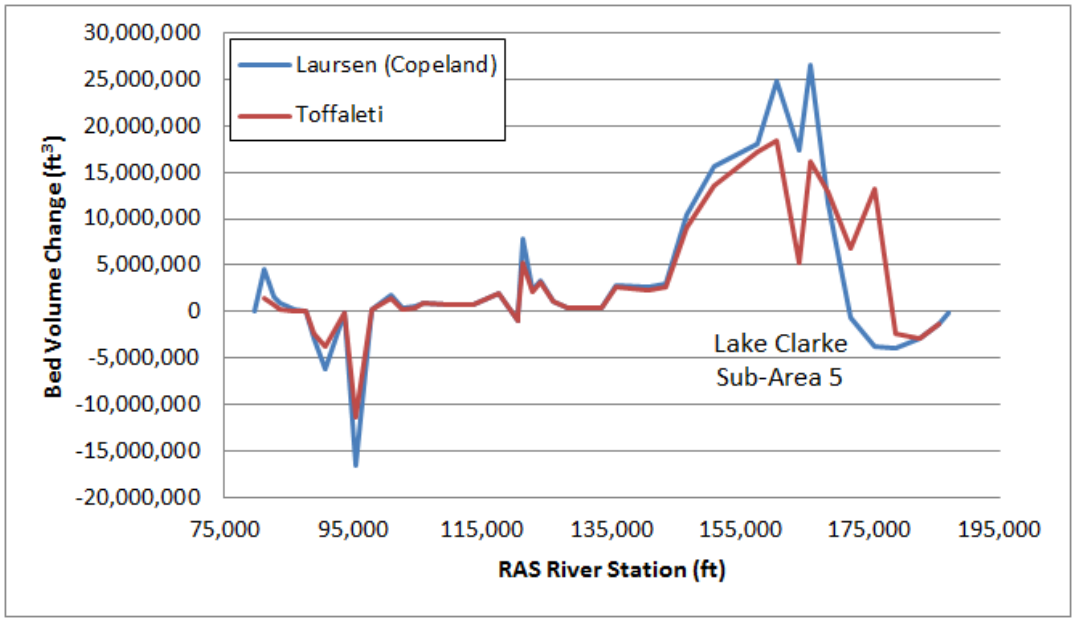

Figure 3.8. Modeled Bed Volume Change 1 January 2008 – 30 August 2013: Laursen (Copeland) vs. Toffaleti

The model was calibrated starting with Lake Clarke's sub-area 5 and working in the downstream direction. Initially, far too much sediment deposited in sub-area 5. This was remedied by reducing the max erodible bed depth at the upstream end of Lake Clarke, near the gage, where the bed is primarily exposed bedrock and some boulders (Zarr, 2016), and removing sediment coarser than fine sand (0.25 mm)

from the inflowing load at the upstream boundary. While it is likely that some coarser material does enter the reservoir system during large events, an analysis of unmeasured bedload transport using the Colby Method (Colby, 1957) resulted in highly unreasonable values, suggesting that coarse material is very limited. Further, the sediment gradations developed by Hainly et al. (1995) were based on samples collected at Harrisburg, PA, and it is likely that much of the coarse sediment which would otherwise be supplied to the model reach is trapped by York Haven Dam, located approximately 12 miles upstream of Marietta. By reducing the amount of coarse sediment scoured or imported at the upstream end of the model, more material was transported downstream, better reflecting observed volume changes. Also, an erosion channel of the shape and size of the main channel was input within sub-area 5, in the deeper, island-free region which conveys the majority of flow during most events. This new feature in HEC-RAS 5.0, which translates parameters from the Erosion Bed Change Option into a simplified channel evolution model and erodes sediment in the shape of a trapezoidal channel, helps mimic the lateral variation in geomorphic changes within the confines of a one-dimensional hydraulic model. Finally, the Manning's *n* value was decreased slightly in the main channel to increase conveyance. While the effects were moderate, these changes helped concentrate the flow and focus the effects of shear stress in the main channel, while still allowing for some deposition near the islands.

Overall, the model initially under predicted deposition for the system as a whole, though results varied by sub-area. To increase deposition, the sediment loading at Marietta was increased by 20-30% at various flows. This resulted in loading values still well within the range of scatter in the observed loading. Figure 3.9 shows a logarithmic plot of sediment load by discharge at Marietta, and presents a comparison of the final rating curve used in the calibrated model with the initial rating curve fit to the observed data and the rating curve used in the HEC-6 model by Hainly et al. (1995).

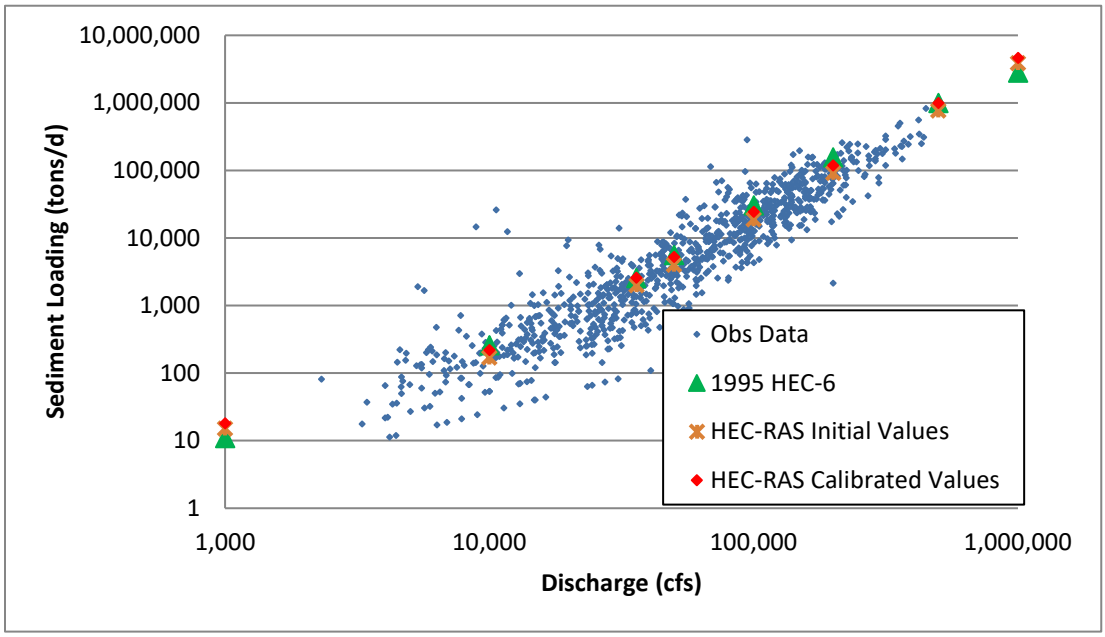

Figure 3.9. Susquehanna Sediment Rating Curve at Marietta, PA

In addition, the effects of seasonal and flow roughness changes were limited to the upstream section of Lake Clarke, where the bed is primarily comprised of bedrock protrusions and boulders, flows are relatively shallow, and roughness values are likely more sensitive to environmental changes. By increasing the amount of sediment entering the system and by decreasing the effects of artificial sinks and sources produced by some roughness factors, more sediment was distributed and deposited in areas where it was needed. Finally, hybrid bed gradations were created for many cross-sections, with the percent clay and cohesive parameters adjusted to promote or resist scour. The changes were relatively small: increases or decreases in clay composition of less than 4 percent of the total sample, and cohesive parameters limited to the range measured in the Sedflume analysis of Conowingo sediments. Final Manning's *n* values chosen for the main channel ranged from 0.023 to 0.029, and values in the overbanks and islands ranged from 0.03 to 0.1.

Overall, the calibration process was largely successful and the modeled net volume change for each reservoir as a whole fell within the target range of the observed values. While it was not possible to fully reverse the longitudinal sedimentation trends in the two reservoirs using justifiable changes to the boundary conditions, significant gains were made. For example, the net excess deposition in Lake Clarke's sub-area 5 was reduced by nearly 65%.

3.3 Model Verification

Following the calibration process, the model was re-run using a simulation period extending from 1 January 2008 to 15 October 2015. Modeled bed volume change results were evaluated from 30 August 2013 through 15 October 2015, and compared with the observed volume changes for the same period to verify the

model's performance. This period was characterized by unusually low flows, with no large events, which provided a good contrast to the calibration period.

While the model performed fairly well from the outset, an iterative calibration process was required to further balance differences between the two periods and achieve modeled volume changes within the target ranges for both reservoirs. The percentage of fines in the Conestoga River and Pequea Creek inflowing loads was increased slightly, to shift the bulk of deposition further downstream within Lake Aldred, and the sediment loading for Pequea Creek was increased by 10-20 percent at various flows. Appendix B presents the final Manning's *n* and sediment input values used in the final verified model.

Table 3.2 presents the modeled bed volume changes for both reservoirs for both the calibration and verification periods.

Table 3.2. Modeled Volume Change. Positive values indicate net deposition while negative numbers indicate net scour.

		Modeled Volume Change (ft^3)	
		2008-2013	**2013-2015**
Lake Clarke	Sub-area 5	15,093,925	5,903,480
	Sub-area 4	83,550,725	21,159,668
	Sub-area 3	55,566,716	13,799,056
	Sub-area 2	12,465,943	3,426,725
	Sub-area 1	13,536,185	2,418,402
	Total	180,213,494	46,707,331
Lake Aldred	Sub-area 3	3,523,891	1,645,122
	Sub-area 4	-466,890	1,219,095
	Sub-area 5	-8,136,708	63,595
	Sub-area 6	-850,882	829,936
	Total	-5,930,589	3,757,748

Figure 3.10 shows a comparison of modeled cumulative bed volume change and target changes in the calibration sub-areas used for Lake Clarke, and Figure 3.11 shows the equivalent comparison for Lake Aldred sub-areas.

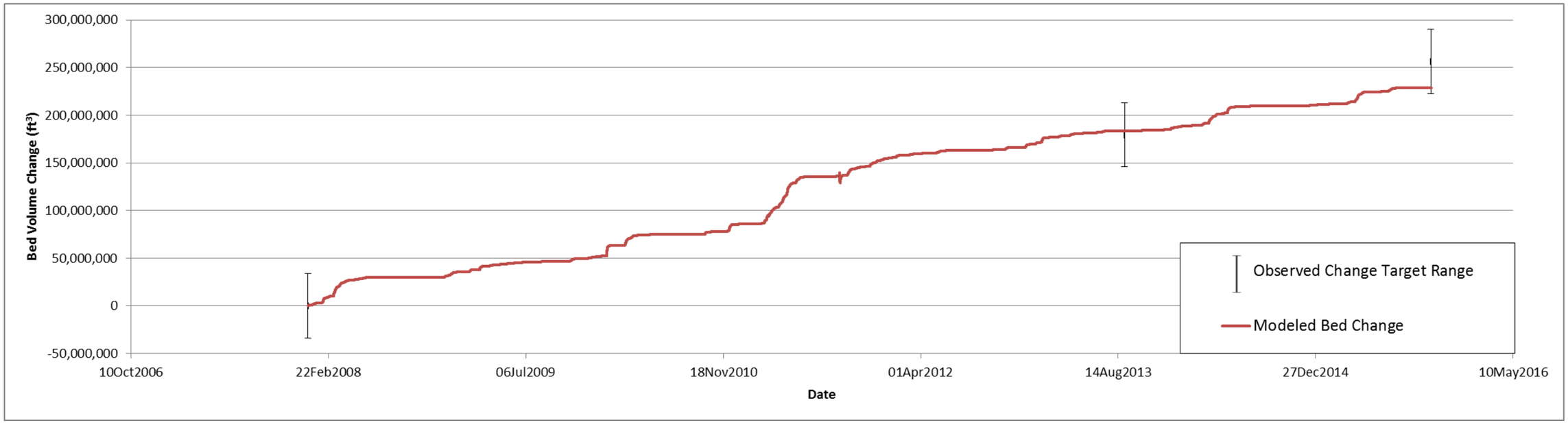

Figure 3.10. Observed vs. Modeled Cumulative Volume Change: Lake Clarke Sub-Areas 1-5, January 2008 – October 2015

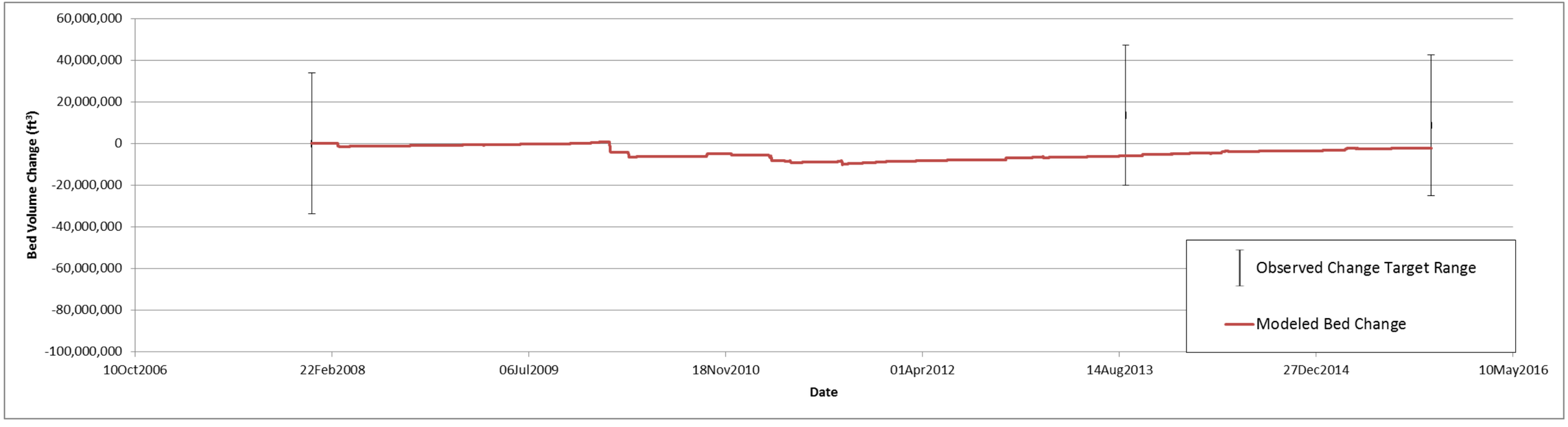

Figure 3.11. Observed vs. Modeled Cumulative Volume Change: Lake Aldred Sub-Areas 3-6, January 2008 – October 2015

4 SEDIMENT MODEL RESULTS

After the model was calibrated and verified, four production runs were executed to simulate four historic flow events not already included in the simulation: April 1993, January 1996, September 2004 (Hurricane Ivan), and June 2006. In each case, one of the four sets of flood hydrographs was added to the ends of the flow time series for the model's upstream boundary and tributary inflows, to simulate the effects of a hypothetical large event given the reservoirs' states in October 2015. The purpose of the production runs was to augment the number of sediment output data at very large flows, for the purpose of strengthening the rating curve fits at higher flows.

Sediment rating curves were created for three locations: the Marietta gage, Safe Harbor Dam, and Holtwood Dam. The sediment mass transport for the 12 particle size classes was aggregated into three classes—sand and gravel, silt, and clay—as requested for use in the Phase 6 Chesapeake Bay Watershed Model. Transport rates for each size class were then plotted versus discharge. The results for each location illustrated aspects of both model and system behavior.

Scatter of results increased in the downstream direction, due in part to the rigid input sediment transport curves applied at the boundaries, but also due to the effects of storage and other natural system factors. Scatter at large flows was more pronounced for sands than for silts and clays, and a clear pattern of hysteresis was visible for individual storm events. Figure 4.1 shows the hourly mass transport results, aggregated into the three size classes, for the Holtwood Dam location. The green points furthest to the right of the plot track the modeled progression of sand transport during Tropical Storm Lee in September 2011. Modeled transport was much greater on the rising limb of the storm than on the falling, likely due to both the asynchronous peaking of the tributaries and mainstem flows and the reduction in applied bed shear stress on the falling limb. While the scatter and hysteresis visible in the silt and clay transport at lower flows appear more significant due to the logarithmic scale, the magnitude of the variance is actually much smaller than that at larger flows. For example, while silt and clay transport rates at low flows vary by about 10,000 tons/day or less for a given discharge, modeled sand transport rates at the highest flows vary by more than 350,000 tons/day for a given discharge.

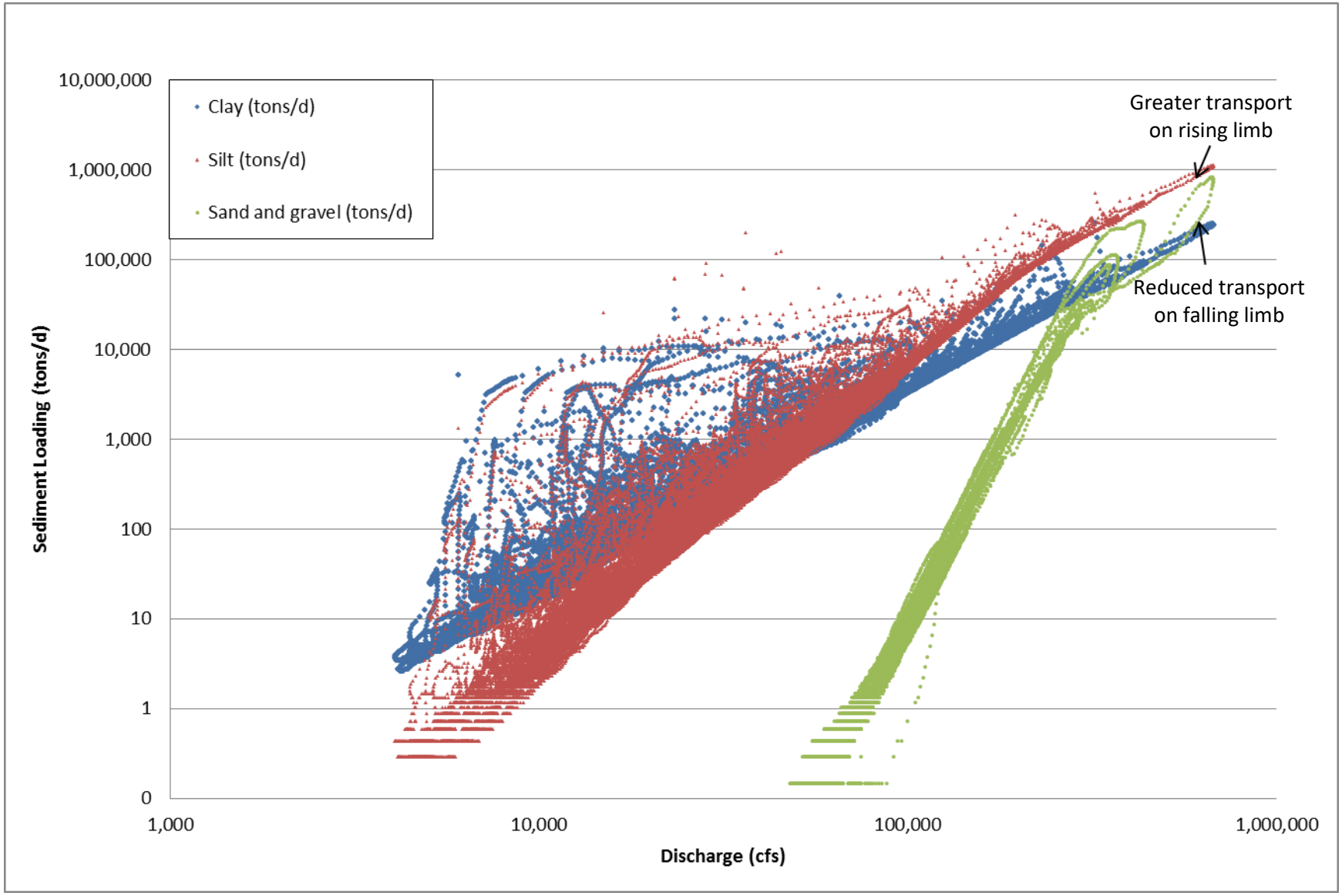

Figure 4.1. Modeled Hourly Sediment Mass Transport vs. Discharge at Holtwood Dam. Each point represents a given hourly flow paired with the associated sediment load for that hour (in units of tons/day)

Piecewise rating curves were fit to daily mass transport data for each particle size class and location, and tabulated transport rates were developed for 29 discharges ranging from 5,000 to 1,000,000 cfs. Plotted rating curves and tables for each location are presented in Appendix C.

While the rating curves were ultimately developed for use in the Chesapeake Bay Watershed Model, comparison of the curves for each location gave additional insights into modeled results. Appendix D presents separate plots of sand, silt, clay and total export for all three sites, with the individual rating curves overlain to facilitate comparison.

A direct visual mass balance is not possible using the three curves alone, for two primary reasons. First, the three locations seldom experience the same discharge simultaneously, and the rating curves do not themselves represent temporal offsets. Second, a true mass balance for Lake Aldred would require explicit representation of all sediment inputs and outputs for the reservoir, and while the rating curves do represent the inputs and outputs at Safe Harbor and Holtwood Dams, respectively, they do not allow for a parsing between tributary loading and reservoir bed scour. Despite these caveats, the relative values of the overlain curves do reflect generally-expected behavior for the reservoirs.

For all particle classes, loading was higher at the Marietta gage at low flows than at Holtwood Dam, indicating net deposition in the system. Conversely, transport was greater at the two dams than at the Marietta streamgage for higher flows, indicating net scour in the system.

5 MODEL LIMITATIONS AND RECOMMENDATIONS

Several key assumptions should be noted in order to understand the modeled results.

First, it is important to understand the limitations of the model itself. While HEC-RAS version 5.0 offers many advantages over previous HEC models developed for the same reach, the model used for the current project was one-dimensional, and as such was limited in its ability to capture the effects of some two-dimensional flow dynamics. Both reservoirs feature islands and other areas with dynamic bathymetric features that vary two-dimensionally. Many zones of scour and deposition were observed in each sub-area, often in the same cross-section. As a one-dimensional model, HEC-RAS was unable to directly simulate bedforms and their effects on channel roughness and flow distribution, and only represented lateral variation in deposition and/or scour using simplified approaches. While the best available methods and data were used in the model's development, it was neither possible nor reasonable to fully capture the effects of all channel features, and the modeling effort's goal was to represent general trends rather than exact values for each sub-area. While the available data do not at present support the application of a reliable two-dimensional sediment transport model for the upper reservoirs for the 2008-2015 simulation period, this option may be more practical in the future.

In addition to the model itself, the availability and quality of the input geometry represent sources of uncertainty in the results. The method of calibrating to bed volume changes necessitated that calibration and verification periods (and, by proxy, the number and magnitude of large events included in the simulation) be determined based on the availability of historical bathymetric data; unfortunately, very few datasets were available for the two reservoirs. The 2008 channel geometry was based on Langland and Koerkle's HEC-RAS model (2014), which itself drew from a number of sources with varying levels of detail and accuracy. The calculated volume changes were subject to uncertainties based on the methods used and the quality of the bathymetric data. The high-density survey data collected by Gomez and Sullivan in 2013 and 2015 represent a significant improvement in both coverage and quality over the bathymetric data used for development of the 2008 geometry, and the availability of future, similarly-high-density bathymetric data may allow for more accurate sediment transport modeling.

Another limitation to model development was the lack of dam operations data for Safe Harbor and Holtwood Dams. While the two structures are largely run-of-river for flows over 110,000 cfs, and rating curves were developed based on reasonable assumptions about gate and power plant operations, it was not possible to fully simulate the effects of peaking schedules, gate operations, and operator judgment. Adding time series of observed pool elevations would improve the model's ability to

accurately represent the structures' historic impacts on flow and sediment discharge.

The relative paucity of large storm events limited the reliability of the sediment output rating curves at very high discharges. Even with the addition of the production runs, the largest modeled output discharge was approximately 660,000 cfs, so the sediment output values for discharges greater than 600,000 cfs were based on projected curves fit to data at lower discharges. Those curves are subject to uncertainty which would only be reduced by modeling larger flows, which itself would require additional input data and model calibration.

Finally, the hysteresis and increased variance in modeled loading at high discharges also limited the usefulness of the rating curves during extreme events. In reality, sediment transport is a function of many variables, so it was not possible to fully capture the reservoirs' behavior using rating curves dependent solely on discharge. In an effort to evaluate the curves' ability to represent longer-term changes, a mass balance was performed on a monthly basis to compare modeled mass changes in each reservoir with expected mass change calculated using the modeled flow time series and the sediment rating curve at each location. (Tributary inflows were also included in the mass balance.) Appendix E presents the results of the mass balance comparison.

The rating curves appeared to be good representations for Lake Clarke, especially for silts and sands. The lake essentially functioned as a pass-through pipe for clays at most discharges, and while slight differences in the clay rating curves at Marietta and Holtwood produced small differences in modeled and calculated clay transport, the magnitude of bed changes due to clay were very small relative to the other particle sizes.

The rating curves did not appear to perform quite as well for Lake Aldred, due to a few reasons. First, the overall magnitude of the bed changes in Lake Aldred was much smaller—Lake Clarke saw consistent and significant deposition over the simulation period, while Lake Aldred alternated between periods of smaller net scour and deposition. Because of this, the percentage difference in monthly mass change calculated by the two methods for Lake Aldred was often very large, even though the magnitude of the difference between the results was often similar to those calculated for Lake Clarke. Also, the discharge-based rating curves represented the modeled sediment transport better in Lake Clarke than in Lake Aldred, given the greater scatter in the modeled sediment transport data for the latter. This is especially true at the upper end of discharges for sand. Note that the month with the greatest discrepancy between the two methods, September 2011 (see Appendix E), corresponds to the period with the largest storm event in the simulation as shown in Figure 4.1. Due to the large variation in sand transport during the rising and falling limbs near the peak of the hydrograph, along with the disproportionate importance of that flow event, sand transport in September 2011

was not represented as well by the rating curve as other sediment size classes and time periods.

6 SUMMARY AND CONCLUSIONS

WEST Consultants, Inc. was contracted by Exelon Corporation to develop a one-dimensional HEC-RAS 5.0 sediment transport model for Lakes Clarke and Aldred on the Lower Susquehanna River, as part of a multi-model initiative. The goal of the modeling effort was to improve understanding of inter-reservoir sediment fluxes, in lieu of measured sediment data, and to provide enhanced inputs for other models.

The HEC-RAS model applied gaged sediment and flow records, sediment core data, and a variety of other inputs to replicate sediment volume change in the two reservoirs between 2008 and 2013, a period characterized by several large storm events. A verification period from 2013 to 2015 validated the model's performance during a time characterized by lower flows. The calibrated model successfully simulated bed changes for both reservoirs and time periods, within target ranges defined by survey equipment accuracy, and predicted both deposition and scour processes at varying discharges and reservoir states.

A time series of discharge and sediment loading at Holtwood Dam was provided to HDR for use as input to their three-dimensional Conowingo Pond Mass Balance Model. Additionally, the model results were used to develop discharge-based sediment rating curves for three particle size classes (sand, silt, and clay) at three locations (Marietta, PA; Safe Harbor Dam; and Holtwood Dam), to aid in parameterization of the Chesapeake Bay Watershed Model by other researchers. While the simplified rating curves do not fully capture the modeled sediment transport dynamics, they do represent substantial improvement over previously-available data.

7 REFERENCES

Colby, B. R., 1957. Relationship of Unmeasured Sediment Discharge to Mean Velocity. *Eos, Transactions American Geophysical Union,* 38(5), pp. 708-717.

Edwards, R. E., 2006. *Comprehensive Analysis of the Sediments Retained Behind Hydroelectric Dams of the Lower Susquehanna River,* Harrisburg: Susquehanna River Basin Commission.

Exelon, 2012. *Final Study Report, Sediment Introduction and Transport Study RSP 3.15,* s.l.: FERC Project Number 404. Prepared by URS Corporation, Gomez and Sullivan Engineers.

Hainly, R. A., Reed, L. A., Flippo, Jr., H. N. & Barton, G. J., 1995. *Deposition and Simulation of Sediment Transport in the Lower Susquehanna River Reservoir System,* Lemoyne: U.S. Department of the Interior, U.S. Geological Survey.

Hirsch, R. M., 2012. *Flux of Nitrogen, Phosphorus, and Suspended Sediment from the Susquehanna River Basin to the Chesapeake Bay during Tropical Storm Lee, September 2011, as an Indicator of the Effects of Reservoir Sedimentation on Water Quality,* Washington, D.C.: U.S. Geological Survey.

Langland, M. J., 2009. *Bathymetry and Sediment-Storage Capacity Change in Three Reservoirs on the Lower Susquehanna River, 1996-2008,* New Cumberland: U.S. Geological Survey.

Langland, M. J. & Koerkle, E. H., 2014. *Calibration of a One-Dimensional Hydraulic Model (HEC-RAS) for Simulating Sediment Transport through Three Reservoirs, Lower Susquehanna River Basin, 2008-2011, Lower Susquehanna River Watershed Assessment, Phase 1, Appendix A with 3 Attachments,* Washington, D.C.: U.S. Department of the Interior, U.S. Geological Survey.

MDNR, 2014. *Quarterly Meeting Summary for April 30, 2012, Lower Susquehanna River Watershed Assessment, Phase 1, Appendix I-6,* Baltimore, MD: Maryland Department of Natural Resources.

Ott, A. N., Takita, C. S., Edwards, R. E. & Bollinger, S. W., 1991. *Loads and Yields of Nutrients and Suspended Sediment Transported in the Susquehanna River Basin, 1985–1989,* Harrisburg: Susquehanna River Basin Commission, Resource Quality Management and Protection Division.

Partheniades, E., 1962. *A Study of Erosion and Deposition of Cohesive Soils in Salt Water.* s.l.:Berkeley Ph.D. Dissertation.

Porse, N. C., 2010. Taking Holtwood into the Next Century. *Hydro Review,* 29(4), p. 8.

Reed, L. A. & Hoffman, S. A., 1996. *Sediment Deposition in Lake Clarke, Lake Aldred, and Conowingo Reservoir, Pennsylvania and Maryland, 1910-93 ,* Lemoyne: U.S. Geological Survey.

Safe Harbor Water Power Corporation, n.d.. *Estimated Levels of Lake Aldred at Holtwood Dam.* [Online]
Available at: http://www.shwpc.com/includes/hd_levels.htm
[Accessed May 2016].

Safe Harbor Water Power Corporation, n.d.. *Facts & Figures.* [Online]
Available at: http://www.shwpc.com/facts_figures.html
[Accessed May 2016].

Scott, S.H. & Sharp, J.A., 2014 (February 2014 draft). *Sediment Transport Characteristics of Conowingo Reservoir, Attachment B-2: Sedflume Erosion Data and Analysis,* ERDC: U.S. Army Corps of Engineers.

SRBC, n.d.. *Sediment and Nutrient Assessment Program (SNAP).* [Online]
Available at: http://www.srbc.net/programs/cbp/nutrientprogram.htm
[Accessed December 2015].

Sullivan, T., 2016a. *Personal Communication.* s.l.:Gomez and Sullivan Engineers.

Takita, C. S. & Edwards, R. E., 2001. *Nutrients and suspended sediment transported in the Susquehanna River Basin, 2000, and trends, January 1985 through December 2000,* Harrisburg: Susquehanna River Basin Commission.

USACE, 2016a. *HEC-RAS River Analysis System Hydraulic Reference Manual Version 5.0,* Davis: United States Army Corps of Engineers.

USACE, 2016b. *HEC-RAS River Analysis System User's Manual, Version 5.0,* Davis: U.S. Army Corps of Engineers.

USEPA, 2010. *Chesapeake Bay TMDL Document.* [Online]
Available at: https://www.epa.gov/chesapeake-bay-tmdl/chesapeake-bay-tmdl-document
[Accessed May 2016].

USGS, 2016a. *USGS Water Data for USA.* [Online]
Available at: http://waterdata.usgs.gov/nwis
[Accessed December 2015].

USGS, 2016b. *USGS Sediment Data Portal.* [Online]
Available at: http://cida.usgs.gov/sediment/
[Accessed December 2015].

Weissman, D., 2016. Talen Closes Popular Lancaster Properties Near Holtwood Dam. *York Dispatch*, 29 April.

Zarr, L., 2016. *Personal Communication.* s.l.:U.S. Geological Survey, Pennsylvania Water Science Center.

Zeff, M. L., 2016. *Personal Communication.* s.l.:AECOM.

APPENDIX A: EXAMPLES OF MEASURED PHYSICAL VS. COHESIVE SOIL PARAMETERS

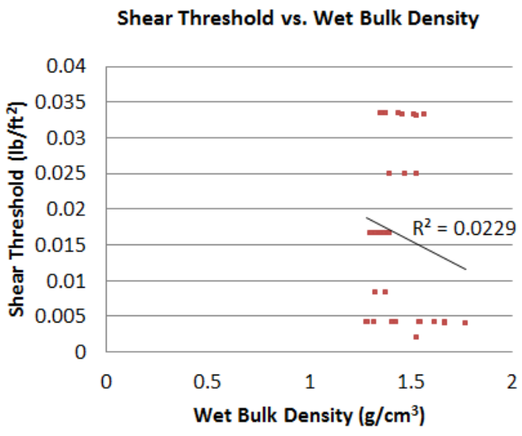

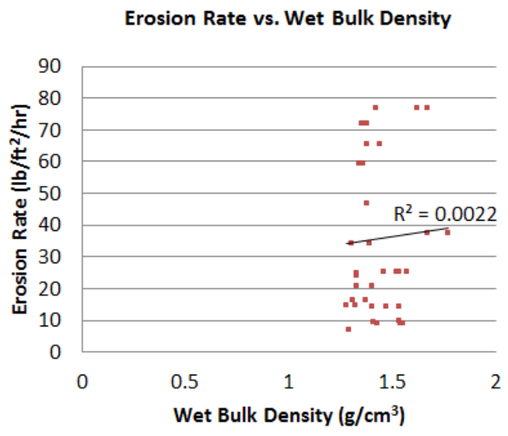

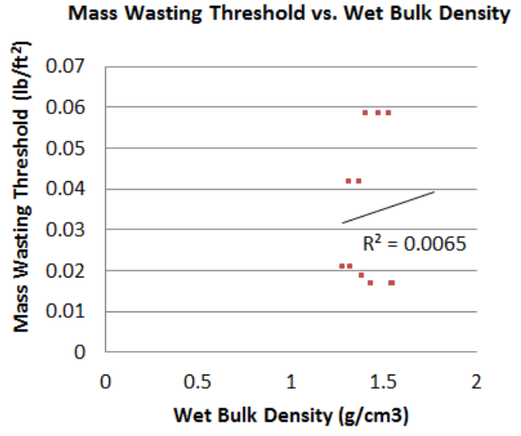

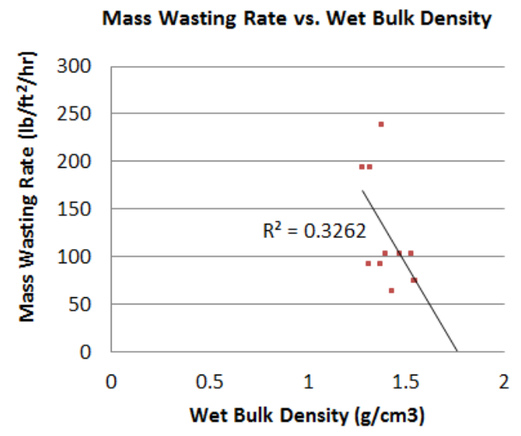

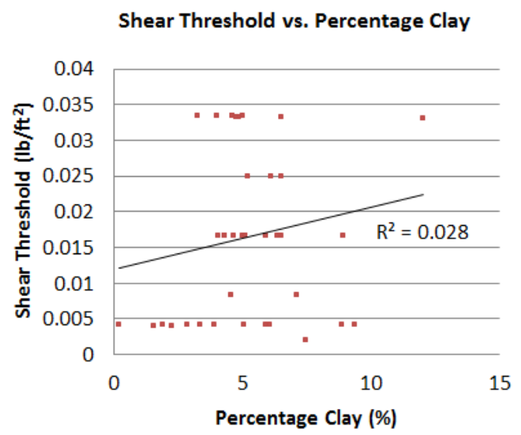

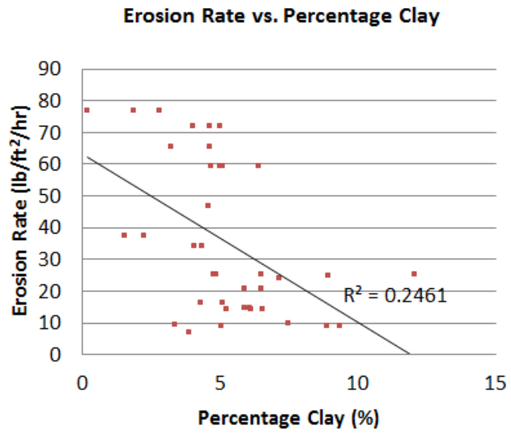

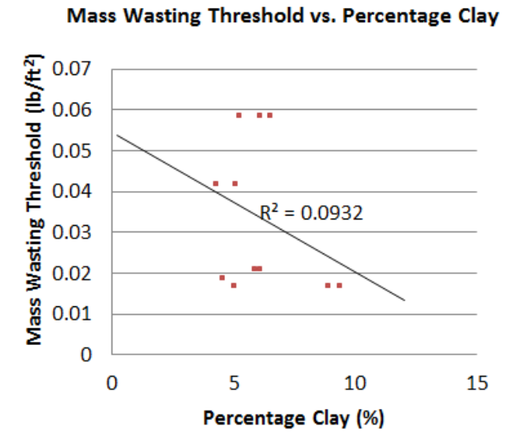

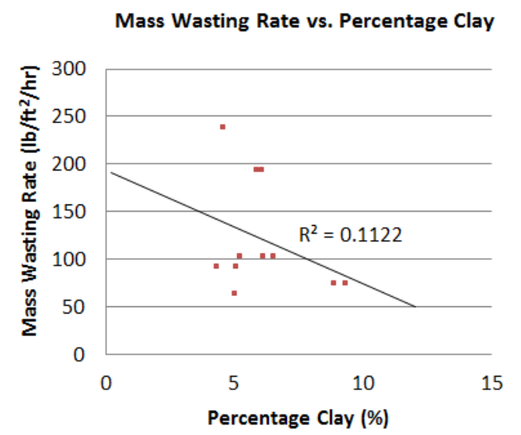

APPENDIX B: FINAL MANNING'S *N* AND SEDIMENT MODEL INPUTS

Horizontal Variation in Manning's *n* Values Used in Final Calibrated Model (Channel Indicated with Blue Background)

Reservoir	River Station (ft)	n #1	n #2	n #3	n #4	n #5	n #6	n #7
Clarke	187225.3	0.1	0.027	0.1				
Clarke	185640.9	0.1	0.04	0.05	0.029	0.1		
Clarke	182695.5	0.1	0.04	0.1	0.029	0.05		
Clarke	179019.5	0.1	0.04	0.1	0.026	0.04		
Clarke	175574.5	0.04	0.029	0.04				
Clarke	171968.3	0.04	0.025	0.04	0.1			
Clarke	168449.8	0.1	0.04	0.023	0.1			
Clarke	165660.4	0.1	0.023	0.08				
Clarke	164038	0.1	0.023	0.08				
Clarke	160414.1	0.1	0.023	0.04	0.08			
Clarke	157477.8	0.1	0.023	0.08				
Clarke	150842.3	0.1	0.1	0.025	0.04	0.08		
Clarke	146692	0.1	0.025	0.08				
Clarke	143399.1	0.1	0.05	0.025	0.08			
Clarke	140634	0.1	0.05	0.025	0.08			
Clarke	135766.3	0.1	0.05	0.025	0.08			
Clarke	133381.7	0.1	0.05	0.025	0.08			
Clarke	130762.2	0.1	0.05	0.025	0.08			
Clarke	128283.1	0.1	0.05	0.025	0.08			
Clarke	126028.8	0.1	0.05	0.025	0.08			
Clarke	124059.3	0.1	0.05	0.023	0.08			
Clarke	122662.5	0.08	0.05	0.023	0.08			
Clarke	121123.2	0.05	0.023	0.1				
			Safe Harbor Dam					
Aldred	120389.2	0.03	0.029	0.08	0.029	0.1		
Aldred	117482.5	0.1	0.05	0.08	0.029	0.1		
Aldred	113547.5	0.08	0.05	0.08	0.025	0.05	0.08	
Aldred	109917.9	0.1	0.05	0.025	0.08	0.025	0.05	
Aldred	105885.6	0.05	0.025	0.08				
Aldred	104476.3	0.08	0.05	0.025	0.08			
Aldred	102620.9	0.1	0.05	0.025	0.1	0.026	0.08	
Aldred	100738.3	0.1	0.05	0.025	0.06	0.08		
Aldred	97895.57	0.1	0.025	0.08				
Aldred	95287.27	0.1	0.05	0.08	0.025	0.08	0.025	0.08
Aldred	93585.01	0.08	0.025	0.08	0.025	0.08		
Aldred	90606.45	0.08	0.025	0.08	0.025	0.08		
Aldred	88933.34	0.1	0.025	0.08				
Aldred	87555.42	0.08	0.05	0.025	0.08			
Aldred	85854.41	0.1	0.05	0.025	0.08			
Aldred	83655.43	0.08	0.025	0.08				
Aldred	82742.23	0.08	0.025	0.08				
Aldred	81117.9	0.08	0.023	0.08				
Aldred	79676.01	0.08	0.05	0.023	0.08			
			Holtwood Dam					

APPENDIX B: FINAL MANNING'S *N* AND SEDIMENT MODEL INPUTS, CONT'D

Bed Sediment Gradations and Cohesive Erosive Parameters Used in Final Calibrated Model

Grain Class	Size (mm)	Lake Clarke (% Finer)							Lake Aldred (% Finer)			
		A	A-1	B-2	C-1	D-1	E-1	F-1	G	H-1	I-1	J-1
Clay	0.004	4.5	6.8	19.2	32.4	24.9	28.4	20.3	14	18.4	2.3	21.3
VF Silt	0.008	5.5	7.5	25.4	45.5	41	44.9	30.3	18.4	27	3.5	29
F Silt	0.016	7.5	9.3	31.1	55.5	56	57.9	41	24.2	35.4	5.3	39.3
M Silt	0.031	9.5	11.1	39.7	68.5	71.7	71.1	52.5	30	45.6	6.8	50
C Silt	0.0625	11.5	12.8	48.2	83.5	82.3	80.1	60	35	57.8	9.3	60.3
VF Sand	0.125	14	15.1	53.9	97.5	87.7	85.4	66	41	71.4	13.5	70.7
F Sand	0.25	23	23.9	60.8	99.5	93.7	95.4	83	59.6	85.2	29.5	82
M Sand	0.5	66.5	67.1	81.5	100	97.7	99.4	93.8	82	94.8	47.8	92.3
C Sand	1	90	90.4	95.1		99.7	99.6	99.3	96.4	98	60.8	96
VC Sand	2	97	97.2	99.3		100	100	99.8	99.4	98.6	69.8	99
VF Gravel	4	100	100	100				100	100	99.6	77	100
F Gravel	8									100	100	
Particle Erosion Threshold (lb/ft^2)		0.0289	0.0021	0.0334	0.0334	0.0334	0.0334	0.0334	0.0289	0.0167	0.0334	0.0334
Particle Erosion Rate ($lb/ft^2/hr$)		19.8334	76.6792	7.0781	7.0781	7.0781	7.0781	7.0781	19.8	40.0565	7.0781	7.0781
Mass Wasting Threshold (lb/ft^2)		0.0585	0.0167	0.0585	0.0585	0.0585	0.0585	0.0585	0.04178	0.0272	0.0585	0.0585
Mass Wasting Erosion Rate ($lb/ft^2/hr$)		102.4847	238.1479	64.1451	64.1451	64.1451	64.1451	64.1451	102	202.266	64.1451	64.1451
Corresponding Model Cross-Sections		187225.3, 185640.9, 182695.5, 179019.5, 175574.5, 171968.3, 168449.8	165660.4, 164038, 160414.1	157477.8, 150842.3, 146692	143399.1	140634, 135766.3	133381.7, 130762.2, 128283.1, 126028.8	124059.3, 122662.5, 121123.2	120389.2, 117482.5, 113547.5, 109917.9	105885.6, 104476.3, 102620.9, 100738.3, 97895.57, 95287.27	93585.01, 90606.45, 88933.34, 87555.42	85854.41, 83655.43, 82742.23, 81117.9, 79676.01

Maximum Erodible Bed Depth Used in Final Calibrated Model

Reservoir	River Station (ft)	Max Bed Depth (ft)
Clarke	187225.3	0.025
Clarke	185640.9	0.025
Clarke	182695.5	0.025
Clarke	179019.5	0.1
Clarke	175574.5	0.1
Clarke	171968.3	0.5
Clarke	168449.8	0.75
Clarke	165660.4	2.7
Clarke	164038	3.3
Clarke	160414.1	4.7
Clarke	157477.8	5.8
Clarke	150842.3	8.4
Clarke	146692	10
Clarke	143399.1	11.2
Clarke	140634	12.3
Clarke	135766.3	14.2
Clarke	133381.7	15.1
Clarke	130762.2	16.1
Clarke	128283.1	17
Clarke	126028.8	17.9
Clarke	124059.3	18.7
Clarke	122662.5	19.2
Clarke	121123.2	19.8
	Safe Harbor Dam	
Aldred	120389.2	0.1
Aldred	117482.5	0.1
Aldred	113547.5	0.25
Aldred	109917.9	1
Aldred	105885.6	3.2
Aldred	104476.3	3.6
Aldred	102620.9	4.1
Aldred	100738.3	4.6
Aldred	97895.57	5.3
Aldred	95287.27	6
Aldred	93585.01	6
Aldred	90606.45	5.5
Aldred	88933.34	5
Aldred	87555.42	2
Aldred	85854.41	5.5
Aldred	83655.43	9
Aldred	82742.23	9.2
Aldred	81117.9	9.6
Aldred	79676.01	0.1
	Holtwood Dam	

APPENDIX B: FINAL MANNING'S *N* AND SEDIMENT MODEL INPUTS, CONT'D

Mainstem and Tributary Sediment Inflows Used in Final Calibrated Model

Final Marietta River Sediment Inflow Loading

Discharge (10^3 cfs)	1	10	36	50	100	200	500	1,000
Total Load (tons/d)	18	220	2,597	5,258	24,530	119,480	1,000,867	4,666,346
Clay (0.002-0.004 mm)	0.20	0.17	0.17	0.16	0.15	0.14	0.13	0.13
VF Silt (0.004-0.008 mm)	0.18	0.16	0.16	0.16	0.15	0.14	0.13	0.13
F Silt (0.008-0.016 mm)	0.24	0.22	0.22	0.22	0.21	0.20	0.19	0.14
M Silt (0.016-0.032 mm)	0.20	0.17	0.18	0.17	0.16	0.15	0.15	0.14
C Silt (0.032-0.0625 mm)	0.18	0.16	0.16	0.15	0.14	0.14	0.14	0.14
VF Sand (0.0625-0.125 mm)	0.00	0.06	0.10	0.10	0.11	0.11	0.14	0.16
F Sand (0.125-0.25 mm)	0.00	0.05	0.09	0.11	0.12	0.13	0.14	0.16

Final Conestoga River Sediment Inflow Loading

Discharge (cfs)	100	1,000	2,000	5,000	10,000	20,000
Total Load (tons/d)	0.8	235	1,155	6,976	23,706	76,932
Clay (0.002-0.004 mm)	0.31	0.29	0.24	0.22	0.2	0.2
VF Silt (0.004-0.008 mm)	0.24	0.24	0.19	0.19	0.18	0.18
F Silt (0.008-0.016 mm)	0.21	0.21	0.17	0.17	0.16	0.15
M Silt (0.016-0.032 mm)	0.16	0.17	0.15	0.14	0.14	0.13
C Silt (0.032-0.0625 mm)	0.08	0.09	0.12	0.12	0.12	0.12
VF Sand (0.0625-0.125 mm)	0	0.02	0.08	0.09	0.1	0.11
F Sand (0.125-0.25 mm)	0	0	0.05	0.06	0.08	0.09
M Sand (0.25-0.5 mm)	0	0	0.03	0.01	0.02	0.02

Final Pequea Creek Sediment Inflow Loading

Discharge (cfs)	50	200	500	1,000	1,500	2,000	5,000	10,000	50,000
Total Load (tons/d)	0	36	610	4,867	17,677	21,774	52,325	100,944	460,850
Clay (0.002-0.004 mm)	0.29	0.27	0.27	0.21	0.2	0.19	0.17	0.17	0.14
VF Silt (0.004-0.008 mm)	0.24	0.22	0.21	0.17	0.16	0.16	0.15	0.15	0.15
F Silt (0.008-0.016 mm)	0.2	0.21	0.22	0.2	0.18	0.17	0.16	0.15	0.15
M Silt (0.016-0.032 mm)	0.18	0.19	0.19	0.15	0.15	0.15	0.15	0.14	0.14
C Silt (0.032-0.0625 mm)	0.09	0.1	0.1	0.11	0.12	0.12	0.12	0.12	0.13
VF Sand (0.0625-0.125 mm)	0	0.01	0.01	0.08	0.09	0.1	0.11	0.12	0.12
F Sand (0.125-0.25 mm)	0	0	0	0.07	0.08	0.08	0.1	0.11	0.12
M Sand (0.25-0.5 mm)	0	0	0	0.01	0.02	0.03	0.04	0.04	0.05
C Sand (0.5-1 mm)	0	0	0	0	0	0	0	0	0

APPENDIX C: TABULAR AND GRAPHICAL SEDIMENT RATING CURVES

	Marietta Gage (tons/d)			Safe Harbor (tons/d)			Holtwood (tons/d)		
Discharge (cfs)	*Clay*	*Silt*	*Sand*	*Clay*	*Silt*	*Sand*	*Clay*	*Silt*	*Sand*
5,000	19	76	8	6	0	0	4	0	0
10,000	38	157	25	23	5	0	22	5	0
15,000	80	336	65	60	23	0	58	21	0
20,000	137	577	123	112	60	0	120	61	0
25,000	208	877	202	178	135	0	200	118	0
30,000	292	1,235	301	260	230	0	300	202	0
40,000	505	2,166	585	480	538	0	530	470	0
50,000	787	3,448	1,023	776	1,040	0	833	905	0
60,000	1,169	5,129	1,587	1,152	1,785	0	1,216	1,544	0
70,000	1,633	7,175	2,297	1,613	2,821	0	1,682	2,422	1
80,000	2,181	9,596	3,142	2,162	4,193	0	2,235	3,577	2
90,000	2,816	12,401	4,193	2,801	5,951	1	2,879	5,043	4
100,000	3,539	15,598	5,394	3,533	8,142	1	3,616	7,000	9
125,000	5,818	25,794	9,225	5,785	15,819	10	5,885	16,000	55
150,000	8,733	38,905	14,294	8,668	27,232	55	8,794	27,000	270
175,000	12,309	55,069	20,693	12,209	43,115	230	12,378	45,424	1,000
200,000	16,572	74,409	28,506	16,436	64,204	650	16,668	66,080	3,200
225,000	21,548	97,290	38,182	21,370	91,233	1,650	21,692	89,977	8,000
250,000	27,251	123,662	49,579	27,034	120,000	4,500	27,476	116,977	15,000
300,000	40,905	187,283	77,867	40,623	189,478	35,000	38,000	190,000	45,000
350,000	57,663	266,057	114,014	57,342	266,203	78,000	54,219	270,000	81,900
400,000	77,585	360,418	158,464	80,000	367,330	138,032	74,241	365,000	128,000
450,000	100,847	471,368	211,961	103,000	474,000	191,392	98,597	475,000	181,721
500,000	127,475	598,467	274,761	130,000	599,000	255,527	127,691	600,000	247,605
600,000	192,691	884,000	431,444	195,000	886,727	418,657	201,703	897,086	421,463
700,000	272,223	1,216,628	623,709	294,619	1,258,666	632,175	299,463	1,305,928	658,878
800,000	379,098	1,602,149	855,123	411,349	1,707,435	900,421	424,123	1,809,991	968,511
900,000	507,848	2,043,519	1,128,552	553,601	2,236,698	1,227,413	578,798	2,415,709	1,358,771
1,000,000	659,794	2,541,390	1,445,544	723,420	2,849,845	1,616,912	766,581	3,129,130	1,837,852

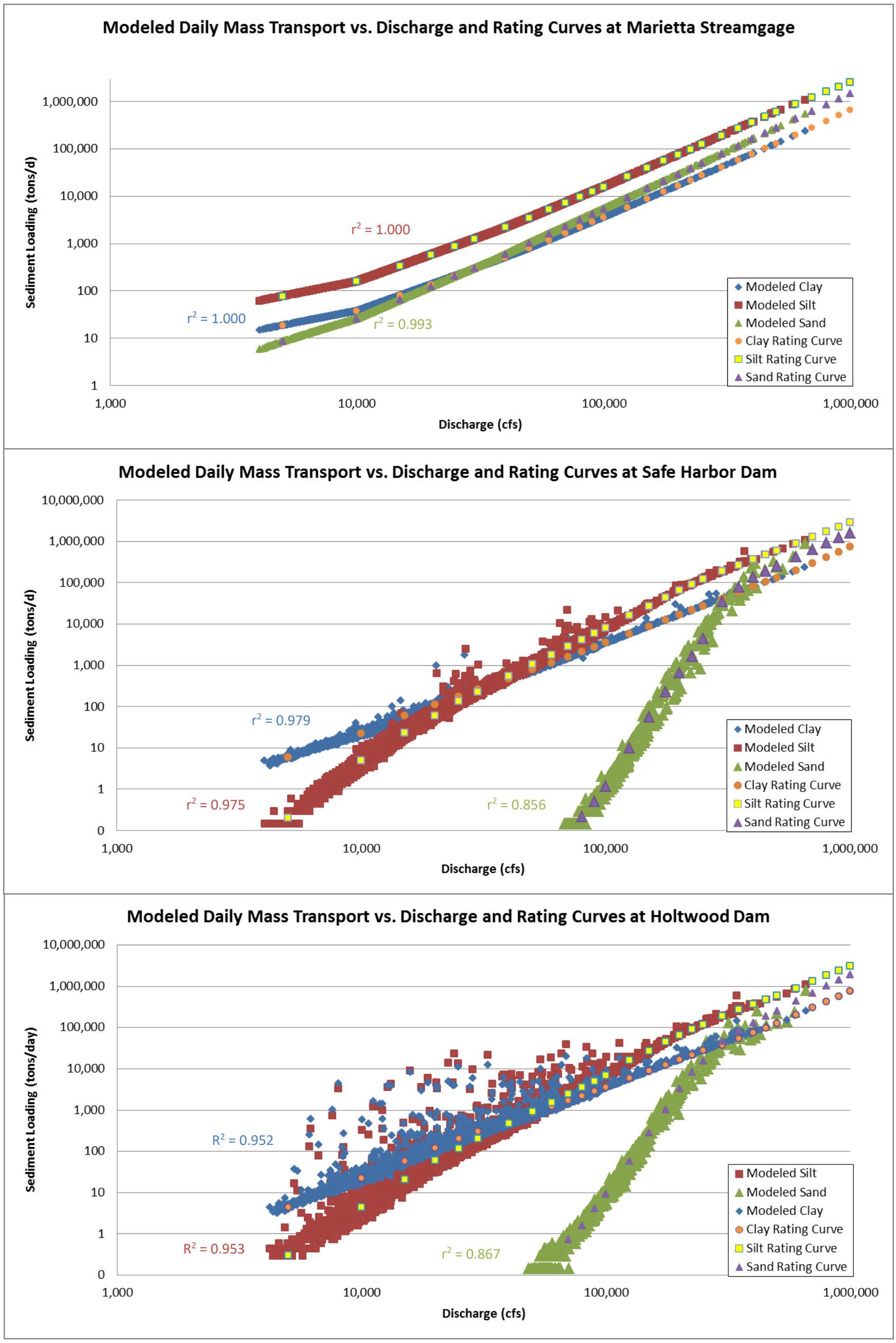
Modeled Daily Mass Transport vs. Discharge and Rating Curves at Marietta Streamgage
Sediment Loading (tons/d)
1,000,000
100,000
10,000
1,000
100
10
1
r² = 1.000
r² = 1.000
r² = 0.993
Modeled Clay
Modeled Silt
Modeled Sand
Clay Rating Curve
Silt Rating Curve
Sand Rating Curve
1,000
10,000
100,000
1,000,000
Discharge (cfs)
Modeled Daily Mass Transport vs. Discharge and Rating Curves at Safe Harbor Dam
Sediment Loading (tons/d)
10,000,000
1,000,000
100,000
10,000
1,000
100
10
1
0
r² = 0.979
r² = 0.975
r² = 0.856
Modeled Clay
Modeled Silt
Modeled Sand
Clay Rating Curve
Silt Rating Curve
Sand Rating Curve
1,000
10,000
100,000
1,000,000
Discharge (cfs)
Modeled Daily Mass Transport vs. Discharge and Rating Curves at Holtwood Dam
Sediment Loading (tons/day)
10,000,000
1,000,000
100,000
10,000
1,000
100
10
1
0
R² = 0.952
R² = 0.953
r² = 0.867
Modeled Silt
Modeled Sand
Modeled Clay
Clay Rating Curve
Silt Rating Curve
Sand Rating Curve
1,000
10,000
100,000
1,000,000
Discharge (cfs)

APPENDIX D: SEDIMENT RATING CURVE COMPARISON

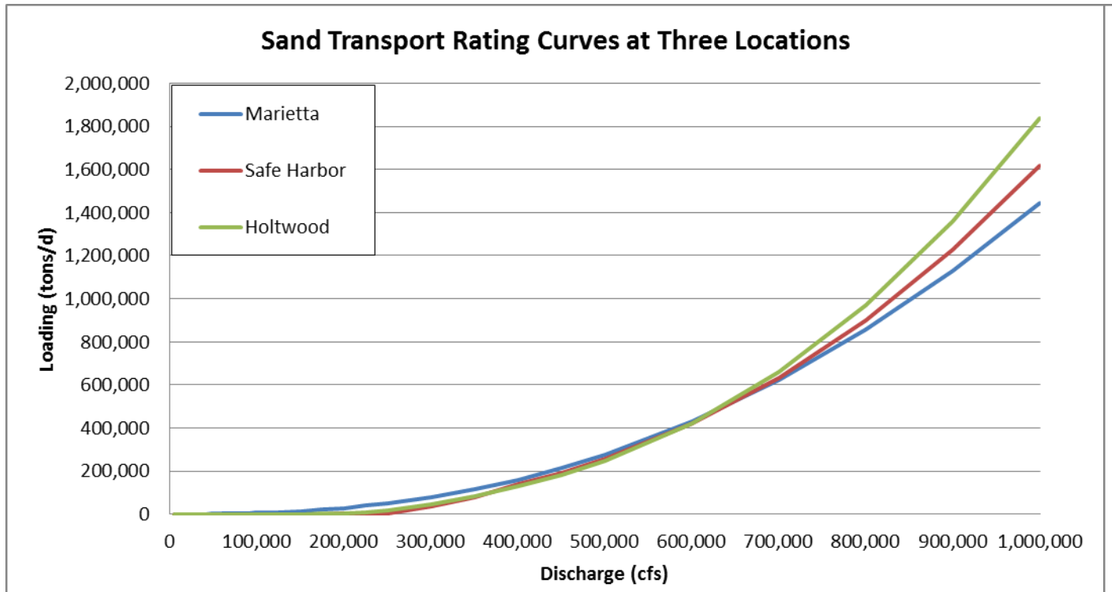

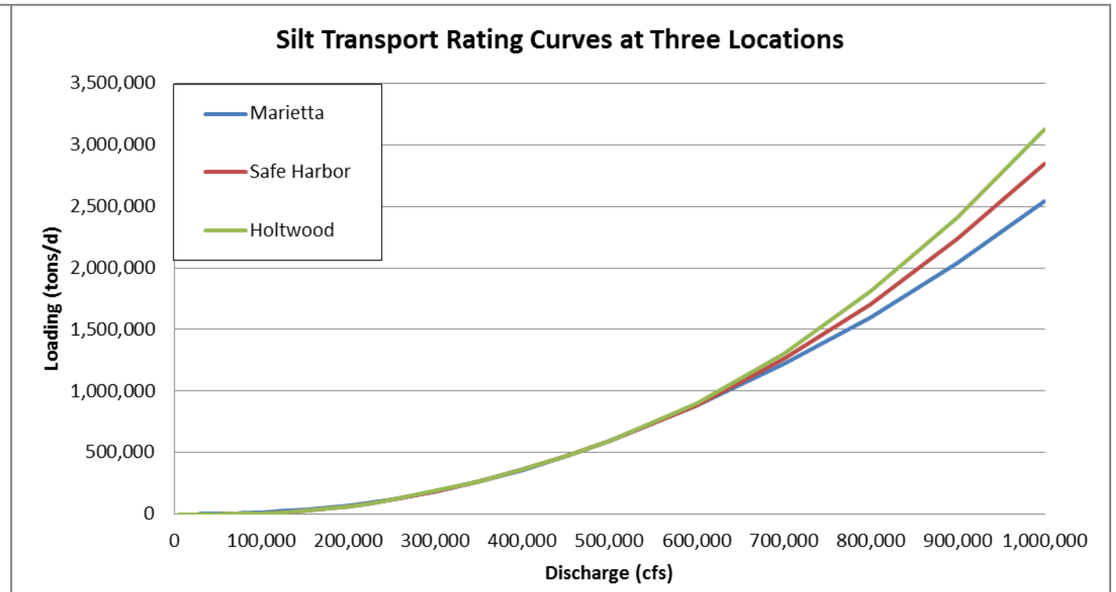

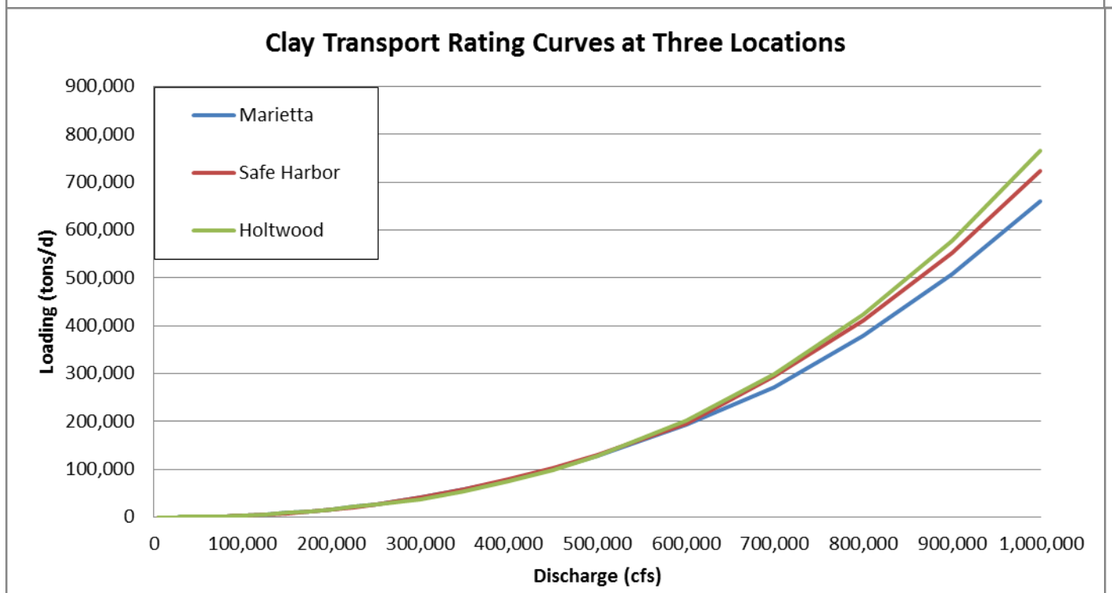

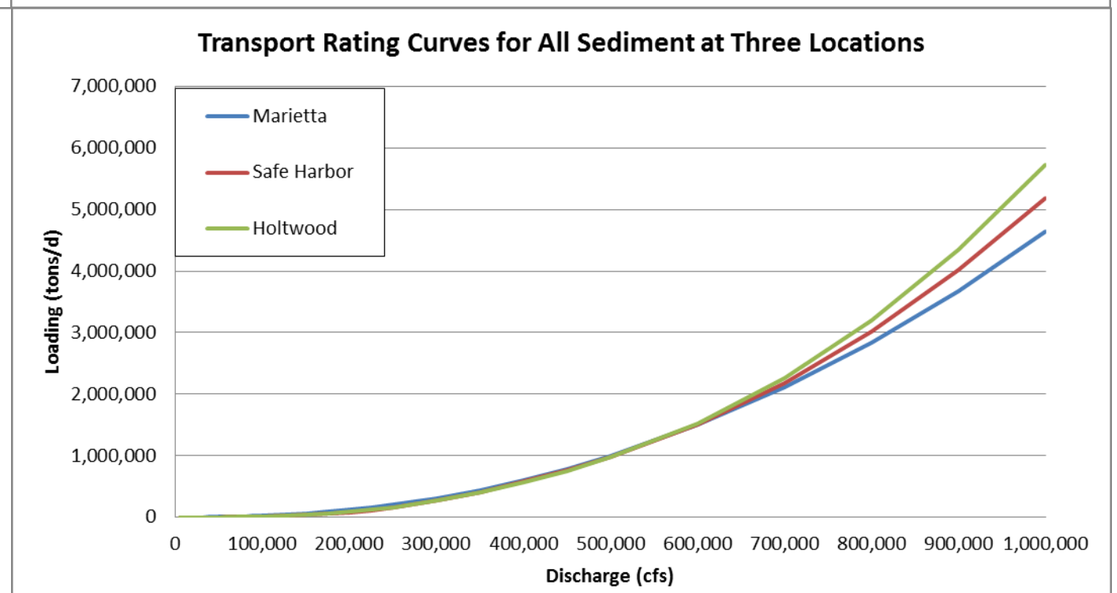

APPENDIX E: MONTHLY MASS BALANCE COMPUTATIONS VS. MODELED MASS CHANGE